NATIONAL ADVISORY COMMITTEE FOR AERONAUTICS

TECHNICAL NOTE 2213

AERODYNAMIC COEFFICIENTS FOR AN OSCILLATING AIRFOIL WITH HINGED FLAP, WITH TABLES FOR A MACH NUMBER OF 0.7

By M. J. Turner and S. Rabinowitz

Chance Vought Aircraft
Division of United Aircraft Corporation

Washington
:tober 1950

NATIONAL ADVISORY COMMITTEE FOR AERONAUTICS

TECHNICAL NOTE 2213

AERODYNAMIC COEFFICIENTS FOR AN OSCILLATING AIRFOIL WITH HINGED FLAP, WITH TABLES FOR A MACH NUMBER OF 0.7

By M. J. Turner and S. Rabinowitz

SUMMARY

Dietze's method for the solution of Possio's integral equation has been used to determine the chordwise distribution of lift on an oscillating airfoil with simple hinged flap in two-dimensional compressible flow (subsonic). The results of these calculations have been used to prepare tables of aerodynamic coefficients for lift, pitching moment (referred to quarter-chord point), and flap hinge moment for a Mach number of 0.7; the motions considered are vertical translation, airfoil rotation about the quarter-chord point, and rotation of the flap about its hinge line.

Aerodynamic coefficients are tabulated for 4 values of τ_R (ratio of flap chord to total chord) and for 12 values of reduced frequency ω_r, covering the range from 0 to 0.7. Results are given for one value of Mach number, $M = 0.7$. Data of this kind have already been presented by Dietze for one value of the ratio of flap chord to total chord, $\tau_R = 0.15$; these results have been checked independently, and calculations have been carried out for three additional values, $\tau_R = 0.24$, 0.33, and 0.42. Certain auxiliary parameters, which will be needed in any further calculations of this type, are presented for future reference.

INTRODUCTION

The fundamental integral equation for the pressure distribution on an oscillating thin airfoil moving at subsonic speed has been derived by Possio in reference 1. Collocation procedures have been used by Possio, Frazer and Skan, and others to obtain lift and moment on an oscillating flat plate. An important contribution has been made by Dietze (see references 2 and 3), who has developed an iterative procedure for numerical solution of Possio's integral equation. This procedure is particularly well adapted to the calculation of aerodynamic loading on an oscillating airfoil with hinged flap.

It has been pointed out correctly by Karp and Weil (reference 4, p. 11) that Dietze's procedure does not properly account for the logarithmic singularity in pressure distribution at the flap hinge. However, for applications in flutter analysis the principal objective is to determine resultant lift and moments rather than pressure distribution. Mathematically exact solutions in closed form are available for the stationary thin airfoil with deflected flap, and it is found that lift and moments obtained by Dietze's iterative procedure are in excellent agreement with theoretically exact values. There is good reason to expect that equally satisfactory results will be obtained for the airfoil with oscillating flap. The existence of the singularity in pressure distribution is a consequence of the sharp corner in the idealized, broken-line profile, and of the associated discontinuity in downwash velocity at the flap hinge. The introduction of a finite cosine series for the downwash is in effect equivalent to a slight modification of the idealized profile by rounding off the corner at the flap hinge.

This work has been performed at Chance Vought Aircraft, under the sponsorship of the Bureau of Aeronautics, Navy Department, in order to provide data for the calculation of compressibility effects in control-surface flutter problems. It has been made available to the National Advisory Committee for Aeronautics for publication because of its general interest.

SYMBOLS

τ_R	ratio of flap chord length to total chord length
R_a	airfoil region in x,z-plane
$\delta_y(x,t)$	vertical displacement of point on idealized profile, positive upward
$\bar{\delta}_y(\xi)$	nondimensional representation of instantaneous chordwise distribution of vertical displacement $\left(\delta_y(x,t) = \frac{l}{2}\,\bar{\delta}_y(\xi)e^{i\omega t}\right)$
l	total chord length
ω	circular frequency
t	time
x	chordwise coordinate

y	vertical coordinate
z	spanwise coordinate
ξ	dimensionless chordwise coordinate $(2x/l)$
$v_y(x,t)$	vertical component of fluid velocity adjacent to airfoil
$g(\xi)$	function representing instantaneous distribution of vertical fluid velocity adjacent to airfoil $\left(v_y(x,t) = g(\xi)e^{i\omega t}\right)$
ω_r	reduced frequency $(\omega l/2V)$
V	velocity of flight
$\gamma(\xi)$	function representing distribution of dipole lines
γ_{inc}	distribution of dipole lines for incompressible flow
$K(s,M)$	kernel of Possio's integral equation
u,v	variables of integration
s	auxiliary variable $\left(\omega_r(\xi - \xi_0)\right)$
M	Mach number
$\mu = 1 - \sqrt{1 - M^2}$	
ρ	air density
$a(x,t)$	lift per unit area
$T(\omega_r)$	function defined by Küssner and Schwarz
$\Delta K(s,M)$	kernel difference $\left(K(s,M) - K(s,0)\right)$
$\Delta K_1(s,M)$	singular part of kernel difference
$\Delta K_2(s,M)$	nonsingular part of kernel difference
k_{ij}	constant occurring in formula for ΔK_1
k_{2n}	coefficient in polynominal representation for ΔK_2

α_i, β_{ik}, $\epsilon_{n\nu}$	coefficients in recursion formulas for solution of Possio's integral equation
ΔP_S	lift force on airfoil strip of width Δz
ΔM_D	pitching moment on airfoil strip of width Δz
ΔM_R	hinge moment on flap for strip of width Δz
q_S	downward displacement of quarter-chord point divided by semichord
q_D	rotation of airfoil, positive in stalling direction
q_R	rotation of flap, positive in stalling direction
c_{gh}, k_{gh}	aerodynamic coefficients, where g, h = S, D, R

BASIC THEORY

A very complete digest of the literature on aerodynamic theory of oscillating airfoils has been presented by Karp, Shu, and Weil in reference 5. Consequently, the basic theory is outlined briefly merely to exhibit the essential features of the computational scheme and to point out certain errors which have been discovered in Dietze's formulas.

The usual assumptions of thin-airfoil theory are adopted, leading to Possio's integral equation for the chordwise lift distribution on the oscillating airfoil. Rectangular coordinates are employed, with the x-axis alined in the direction of the undisturbed flow. The airfoil is replaced by a deformable sheet of zero thickness which, in its undisturbed position, occupies the region R_a

$$-l/2 \leqq x \leqq l/2, \quad y = 0$$

of the x,z-plane.

The lifting surface executes sinusoidal oscillations in which each point moves along a line parallel to the vertical y-axis. Displacements are independent of the spanwise coordinate z, and may be represented in the form

$$\delta_y = \delta_y(x,t) = \frac{l}{2}\,\bar{\delta}_y(\xi)e^{i\omega t}$$

In accordance with the usual convention, it is the real part of equation (1) which has physical significance.

The y-component of velocity of a fluid particle adjacent to the lifting surface is related to δ_y by the equation

$$v_y = \frac{\partial \delta_y}{\partial t} + V \frac{\partial \delta_y}{\partial x} = \frac{\partial \delta_y}{\partial t} + \frac{2V}{l} \frac{\partial \delta_y}{\partial \xi} \tag{2}$$

where $\xi = 2x/l$ and $-1 \leq \xi \leq 1$ inside R_a. From equations (1) and (2) it follows that

$$v_y = g(\xi) e^{i\omega t} \tag{3}$$

where

$$g(\xi) = V\left(i\omega_r \bar{\delta}_y + \frac{d\bar{\delta}_y}{d\xi}\right) \tag{4}$$

where

$$\omega_r = \omega l/2V$$

In Dietze's derivation of the basic integral equation the region R_a is covered with dipole lines of density $V\gamma(x)e^{i\omega t}$ per unit length in the chordwise direction. By equating the vertical velocity induced by the dipole covering to that given by equation (3) the following integral equation is obtained for the determination of γ:

$$g(\xi) = \omega_r \int_{-1}^{1} \gamma(\xi_0) K(s,M)\, d\xi_0 \tag{5}$$

subject to the condition that $\gamma(1)$ shall be finite; the kernel of the integral equation is given by

$$K(s,M) = -\frac{e^{is\lambda M}}{4\sqrt{1 - M^2}} \left\{ H_0^{(2)}(|s|\lambda) - iM \frac{s}{|s|} H_1^{(2)}(|s|\lambda) - i(1 - M^2) e^{-is\frac{\lambda}{M}} \left[\frac{2}{\pi\sqrt{1 - M^2}} \log_e \frac{M}{1 - \sqrt{1 - M^2}} + \int_0^{s\frac{\lambda}{M}} e^{iu} H_0^{(2)}(|u|M)\, du \right] \right\} \tag{6}$$

with

$$s = \omega_r(\xi - \xi_0)$$

$$\lambda = M/(1 - M^2)$$

The lift a per unit area (positive upward) is given by

$$a(x,t) = \rho V \gamma(x) e^{i\omega t} \tag{7}$$

NUMERICAL SOLUTION OF POSSIO'S INTEGRAL EQUATION

Dietze's approximate solution of equation (5) (Possio's integral equation) is of the form

$$\gamma \approx \gamma_{inc} + \gamma_1 + \gamma_2 + \ldots + \gamma_n \tag{8}$$

where γ_{inc} and γ_ν ($\nu = 1, 2, \ldots, n$) are solutions of the integral equations

$$g(\xi) = \omega_r \oint_{-1}^{1} \gamma_{inc}(\xi_0) K(s,0)\, d\xi_0 \tag{9}$$

$$g_\nu(\xi) = \omega_r \oint_{-1}^{1} \gamma_\nu(\xi_0) K(s,0)\, d\xi_0, \quad \nu = 1, 2, \ldots, n \tag{10}$$

and where

$$g_1(\xi) = \omega_r \oint_{-1}^{1} \gamma_{inc}(\xi_0) \left[K(s,0) - K(s,M)\right] d\xi_0 \tag{11}$$

$$g_\nu(\xi) = \omega_r \oint_{-1}^{1} \gamma_{\nu-1}(\xi_0) \left[K(s,0) - K(s,M)\right] d\xi_0, \quad \nu = 2, 3, \ldots, n \tag{12}$$

$$K(s,0) = \lim_{M \to 0} K(s,M)$$

The required solutions of equations (9) and (10) are obtained by the methods of reference 6. Convergence of the process has been proved only for the stationary case. However, computational experience furnishes convincing evidence that the process does converge in the more general case.

It will be observed that Dietze's process requires essentially the solution of a succession of integral equations with kernel $K(s,0)$ from the incompressible problem. The functions $g_\nu(\xi)$ are obtained by direct integration in accordance with equations (11) and (12).

In case $g_\nu(\xi)$ can be represented by a cosine series of form

$$g_\nu(\xi) = V\left(A_0 + 2\sum_{n=1}^{\infty} A_n \cos n\phi\right), \quad 0 \leqq \phi \leqq \pi \tag{13}$$

with

$$\xi = -\cos \phi$$

then it is known from the work of Küssner and Schwarz (reference 6) that

$$\gamma_\nu(\xi) = -2V\left(a_0 \cot \frac{\phi}{2} + 2\sum_{n=1}^{\infty} a_n \sin n\phi\right) \tag{14}$$

where

$$\left.\begin{aligned} a_0 &= \left(\frac{1+T}{2}\right)(A_0 - A_1) + A_1 \\ a_n &= \frac{i\omega_r}{2n}(A_{n-1} - A_{n+1}) - A_n, \quad n \geqq 1 \end{aligned}\right\} \tag{15}$$

and $T(\omega_r)$ is the function of reduced frequency defined in reference 6. The T-function is related to Theodorsen's C-function by the equation $T = 2C - 1$.

In order to facilitate the evaluation of the integral occurring in equation (12) the kernel difference

$$\Delta K(s,M) = K(s,M) - K(s,0)$$

is expressed in the form

$$\Delta K(s,M) = \Delta K_1(s,M) + \Delta K_2(s,M) \tag{16}$$

where

$$\Delta K_1(s,M) = \frac{k_{10}}{s} + k_{11} + k_{12} \log_e |s| + s\left(k_{13} + k_{14} \log_e |s|\right) \tag{17}$$

$$k_{10} = \frac{1}{2\pi}\left(1 - \sqrt{1 - M^2}\right)$$

$$k_{11} = -\frac{1}{4}\left(\frac{1}{\sqrt{1 - M^2}} - 1\right) - \frac{i}{2\pi}\left\{\frac{1}{\sqrt{1 - M^2}}\left[M^2 - \log_e \frac{\gamma M}{2(1 - M^2)}\right] + \log_e \frac{\gamma M}{1 + \sqrt{1 - M^2}}\right\}$$

$$k_{12} = -\frac{i}{2\pi}\left(1 - \frac{1}{\sqrt{1 - M^2}}\right)$$

$$k_{13} = -\frac{1}{2\pi}\left\{-1 + \log_e \frac{\gamma M}{1 + \sqrt{1 - M^2}} + \frac{1}{(1 - M^2)^{3/2}}\left[1 - \frac{3}{4} M^2 - \frac{1}{2} M^4 - \left(1 - \frac{3}{2} M^2\right) \log_e \frac{\gamma M}{2(1 - M^2)}\right]\right\} - \frac{i}{4}\left[1 + \frac{3M^2 - 2}{2(1 - M^2)^{3/2}}\right]$$

$$k_{14} = -\frac{1}{2\pi}\left[1 + \frac{3M^2 - 2}{2(1 - M^2)^{3/2}}\right]$$

$\log_e \gamma = 0.57722$ (Euler's constant)

The nonsingular part $\Delta K_2(s,M)$ is replaced by a polynomial of ninth degree[1]

$$\Delta K_2(s,M) \approx -\sum_{n=2}^{9} k_{2n} s^n \tag{18}$$

whose coefficients are determined separately for each Mach number by fitting the polynomial to tabulated values in the interval $|s| \leqq 1.8$.

Equation (12) may be written in the form

$$g_\nu(\xi) = -\omega_r \oint_{-1}^{1} \gamma_{\nu-1} \, \Delta K(s,M) \, d\xi_0 \tag{19}$$

If it be assumed that

$$\gamma_{\nu-1} = -2V\left(p_0 \cot \frac{\phi}{2} + 2\sum_{n=1}^{\infty} p_n \sin n\phi\right) \tag{20}$$

then it follows that (upon carrying out the required integrals defining g_ν, in accordance with equations (17), (18), and (19) and applying equations (15) to solve equation (10)),

$$\gamma_\nu = -2V\left(q_0 \cot \frac{\phi}{2} + 2\sum_{n=1}^{\infty} q_n \sin n\phi\right) \tag{21}$$

where

$$q_n = q_{1n} + q_{2n} \tag{22}$$

---

[1]Dietze's definition of the approximating polynomial (table 3 of reference 2) differs in sign from that given here. However, it has been found by carefully checking the derivations that the minus sign is required in equation (18) in order to justify the recursion formulas for calculating γ_ν from $\gamma_{\nu-1}$. It is believed that this is merely an error of presentation, since Dietze's numerical results are found to be substantially correct.

and

$$
\left.
\begin{aligned}
q_{10} &= \mu\left(-p_1 + \beta_{00}p_0' + \beta_{01}p_1' + \beta_{02}p_2'\right) \\
q_{11} &= \mu\left(p_1 + \beta_{10}p_0' + \beta_{11}p_1' + \beta_{12}p_2' + \beta_{13}p_2''\right) \\
q_{12} &= \mu\left(p_2 + \beta_{20}p_0' + \beta_{21}p_2' + \beta_{22}p_2'' + \beta_{23}p_3''\right) \\
q_{1n} &= \mu\left(p_n + \alpha_1 p_n' + \alpha_2 p_n'' + \alpha_3 p_n'''\right), \quad n \geq 3 \\
q_{20} &= 2\pi \sum_{\nu=0}^{9} p_\nu' \epsilon_{0\nu} \\
q_{2n} &= (-1)^{n+1} 2\pi \sum_{\nu=0}^{10-n} p_\nu' \epsilon_{n\nu}, \quad n \geq 1
\end{aligned}
\right\} \tag{23}
$$

with

$$
\begin{aligned}
p_0' &= -\frac{1}{2}\left(p_0 + p_1\right) \\
p_1' &= -\frac{1}{2}\left(p_0 + p_2\right) \\
p_n' &= \frac{1}{2n}\left(p_{n-1} - p_{n+1}\right), \quad n \geq 2 \\
p_n'' &= \frac{1}{2n}\left(p_{n-1}' - p_{n+1}'\right), \quad n \geq 2 \\
p_n''' &= \frac{1}{2n}\left(p_{n-1}'' - p_{n+1}''\right), \quad n \geq 3
\end{aligned}
$$

The quantities α_i, β_{ik}, and $\epsilon_{n\nu}$ are defined in the translation of reference 2 (see table 5, p. 28, and tables 6 and 7, pp. 30-32). It was found that the formula for $\epsilon_{0\nu}$ is given incorrectly by Dietze; it should read

$$\epsilon_{0\nu} = \left(\frac{1 + T}{2}\right)\left(\delta_{0\nu} + \delta_{1\nu}\right) - \delta_{1\nu} \tag{24}$$

Presumably this is merely an error in presentation, since, as already noted, Dietze's numerical results have been verified by independent calculations. Numerical values of the parameters α_i, β_{ik} for $M = 0.7$ and reduced frequencies ranging from 0 to 0.7 are given in table I.

EVALUATION OF KERNEL AND KERNEL DIFFERENCE

By making use of the relations among Bessel, Hankel, and Neumann functions and by separating the kernel into real and imaginary parts an expression of the following form is obtained:

$$K(s,M) = K'(s,M) + iK''(s,M) = \frac{-A(s,M)\cos(s\lambda M) + B(s,M)\sin(s\lambda M)}{4\sqrt{1 - M^2}} + i\,\frac{B(s,M)\cos(s\lambda M) - A(s,M)\sin(s\lambda M)}{4\sqrt{1 - M^2}} \tag{25}$$

where

$$\left.\begin{aligned} A = {} & J_0(|s|\lambda) - M\frac{s}{|s|}N_1(|s|\lambda) - \frac{2}{\pi}\sqrt{1 - M^2}\log_e\frac{M}{1 - \sqrt{1 - M^2}}\sin\left(s\frac{\lambda}{M}\right) - \\ & (1 - M^2)\sin\left(s\frac{\lambda}{M}\right)\int_0^{s\frac{\lambda}{M}}\left[\cos u\, J_0(|u|M) + \sin u\, N_0(|u|M)\right]du - \\ & (1 - M^2)\cos\left(s\frac{\lambda}{M}\right)\int_0^{s\frac{\lambda}{M}}\left[\cos u\, N_0(|u|M) - \sin u\, J_0(|u|M)\right]du \\ B = {} & N_0(|s|\lambda) + M\frac{s}{|s|}J_1(|s|\lambda) + \frac{2}{\pi}\sqrt{1 - M^2}\log_e\frac{M}{1 - \sqrt{1 - M^2}}\cos\left(s\frac{\lambda}{M}\right) + \\ & (1 - M^2)\cos\left(s\frac{\lambda}{M}\right)\int_0^{s\frac{\lambda}{M}}\left[\cos u\, J_0(|u|M) + \sin u\, N_0(|u|M)\right]du - \\ & (1 - M^2)\sin\left(s\frac{\lambda}{M}\right)\int_0^{s\frac{\lambda}{M}}\left[\cos u\, N_0(|u|M) - \sin u\, J_0(|u|M)\right]du \end{aligned}\right\} \tag{26}$$

By introducing a new variable of integration

$$v = \frac{M}{\lambda} u$$

equations (26) are transformed into

$$A = J_0(|s|\lambda) - M \frac{s}{|s|} N_1(|s|\lambda) - \frac{2}{\pi}\sqrt{1 - M^2} \log_e \frac{M}{1 - \sqrt{1 - M^2}} \sin\left(s \frac{\lambda}{M}\right) -$$

$$\sin\left(s \frac{\lambda}{M}\right) \int_0^s \left[\cos\left(v \frac{\lambda}{M}\right) J_0(|v|\lambda) + \sin\left(v \frac{\lambda}{M}\right) N_0(|v|\lambda)\right] dv -$$

$$\cos\left(s \frac{\lambda}{M}\right) \int_0^s \left[\cos\left(v \frac{\lambda}{M}\right) N_0(|v|\lambda) - \sin\left(v \frac{\lambda}{M}\right) J_0(|v|\lambda)\right] dv \qquad (27)$$

$$B = N_0(|s|\lambda) + M \frac{s}{|s|} J_1(|s|\lambda) + \frac{2}{\pi}\sqrt{1 - M^2} \log_e \frac{M}{1 - \sqrt{1 - M^2}} \cos\left(s \frac{\lambda}{M}\right) +$$

$$\cos\left(s \frac{\lambda}{M}\right) \int_0^s \left[\cos\left(v \frac{\lambda}{M}\right) J_0(|v|\lambda) + \sin\left(v \frac{\lambda}{M}\right) N_0(|v|\lambda)\right] dv -$$

$$\sin\left(s \frac{\lambda}{M}\right) \int_0^s \left[\cos\left(v \frac{\lambda}{M}\right) N_0(|v|\lambda) - \sin\left(v \frac{\lambda}{M}\right) J_0(|v|\lambda)\right] dv \qquad (28)$$

Numerical values of the following integrals are required:

$$\left.\begin{aligned} I_1(s) &= \int_0^s \cos\left(v\frac{\lambda}{M}\right) J_0(|v|\lambda)\, dv \\ I_2(s) &= \int_0^s \sin\left(v\frac{\lambda}{M}\right) J_0(|v|\lambda)\, dv \\ I_3(s) &= \int_0^s \cos\left(v\frac{\lambda}{M}\right) N_0(|v|\lambda)\, dv \\ I_4(s) &= \int_0^s \sin\left(v\frac{\lambda}{M}\right) N_0(|v|\lambda)\, dv \end{aligned}\right\} \tag{29}$$

The evaluation of I_1 and I_2 can be obtained by numerical integration in a straightforward manner. However, since $N_0(x)$ has a logarithmic singularity at $x = 0$, it is necessary to express I_3 and I_4 in different form. Upon making the substitution (reference 7, pp. 130, 132)

$$\frac{\pi}{2} N_0(x) = J_0(x) \log_e \frac{\gamma x}{2} - B_0(x)$$

where

$$B_0(x) = -\left(\frac{x}{2}\right)^2 + \frac{1+\frac{1}{2}}{(2!)^2}\left(\frac{x}{2}\right)^4 - \frac{1+\frac{1}{2}+\frac{1}{3}}{(3!)^2}\left(\frac{x}{2}\right)^6 + \cdots$$

and integrating by parts, the following equations are obtained:

$$\frac{\pi}{2} I_3(s) = I_1(s) \log_e \frac{\gamma s\lambda}{2} - \int_0^s \frac{I_1(v)}{v} dv - \int_0^s \cos\left(v \frac{\lambda}{M}\right) B_0(v\lambda)\, dv \quad (30)$$

$$\frac{\pi}{2} I_4(s) = I_2(s) \log_e \frac{\gamma s\lambda}{2} - \int_0^s \frac{I_2(v)}{v} dv - \int_0^s \sin\left(v \frac{\lambda}{M}\right) B_0(v\lambda)\, dv \quad (31)$$

It follows from equations (29) that I_1 and I_3 are odd functions, while I_2 and I_4 are even. The integrals occurring in equations (30) and (31) can be evaluated numerically without difficulty; it should be noted that

$$\lim_{v \to 0} \frac{I_1(v)}{v} = 1$$

$$\lim_{v \to 0} \frac{I_2(v)}{v} = 0$$

In computing numerical values of the kernel Dietze has used the tables of Bessel and Neumann functions given in reference 7, which do not permit a satisfactory determination of B_0 since N_0 is tabulated to only four (in some cases three) places. In recalculating the kernel the seven-place tables given in reference 8 have been used.

For evaluation of the integrals I_n the formulas given in reference 9, page 227, have been extended to include fifth differences. These formulas have been used with an interval $\Delta(s\lambda) = 0.05$, and the results have been checked up to $s\lambda = 0.30$ by using an interval $\Delta(s\lambda) = 0.02$. Recalculated values of $K(s,0.7)$, $K(s,0)$, $\Delta K(s,0.7)$, $\Delta K_1(s,0.7)$, and $\Delta K_2(s,0.7)$ are given in table II. These values are found to be in close agreement with those given by Dietze; where differences exist, the new values are believed to be more accurate. In making comparisons it should be noted that Dietze has tabulated $-K(s,M)$.

The coefficients k_{2n} are obtained by fitting a ninth-degree polynomial (see equation (18)) to the tabulated values of ΔK_2 in the

interval $|s| \leqq 1.8$ by the method of least squares. The values obtained in this way for $M = 0.7$ are

$$k_{22} = -0.046728 - 0.045974i$$

$$k_{23} = 0.023019 - 0.023491i$$

$$k_{24} = 0.009818 + 0.052855i$$

$$k_{25} = -0.020228 + 0.003488i$$

$$k_{26} = -0.001040 - 0.021510i$$

$$k_{27} = 0.007272 - 0.000283i$$

$$k_{28} = 0.000053 + 0.003117i$$

$$k_{29} = -0.000997 + 0.000012i$$

Since $|s| = \omega_r(\xi - \xi_0)$ and $|\xi - \xi_0| \leqq 2$ the approximate representation for ΔK_2 is valid for reduced frequencies in the range $0 \leqq \omega_r \leqq 0.9$. Although the values of the coefficients k_{2n} given here differ from those given by Dietze (see translation of reference 2, p. 26), there is reasonable agreement of coefficients for lower powers of s. Also the algebraic signs agree; this gives further indication that Dietze must have introduced a minus sign in his definition of the approximate representation for ΔK_2.

NOTATION FOR AERODYNAMIC LIFT AND MOMENTS

In presenting his numerical results Dietze has introduced representations of lift force and moments involving only real quantities. Complex notation is used in the present report in order to conform more nearly to current American practice; however the essential features of Dietze's notation (translation of reference 3) are retained. Lift and moments on an airfoil strip of width Δz for an airfoil with simple hinged flap are as follows:

$$\left.\begin{aligned}
\Delta P_S &= \pi\rho V^2\left(\frac{l}{2}\right)\Delta z\left[\left(\omega_r{}^2 c_{SS} - k_{SS}\right)q_S + \left(\omega_r{}^2 c_{SD} - k_{SD}\right)q_D + \left(\omega_r{}^2 c_{SR} - k_{SR}\right)q_R\right] \\
\Delta M_D &= \pi\rho V^2\left(\frac{l}{2}\right)^2\Delta z\left[\left(\omega_r{}^2 C_{DS} - k_{DS}\right)q_S + \left(\omega_r{}^2 c_{DD} - k_{DD}\right)q_D + \left(\omega_r{}^2 c_{DR} - k_{DR}\right)q_R\right] \\
\Delta M_R &= \pi\rho V^2\left(\frac{l}{2}\right)^2\Delta z\left[\left(\omega_r{}^2 c_{RS} - k_{RS}\right)q_S + \left(\omega_r{}^2 c_{RD} - k_{RD}\right)q_D + \left(\omega_r{}^2 c_{RR} - k_{RR}\right)q_R\right]
\end{aligned}\right\} \quad (32)$$

where

ΔP_S lift force, positive upward

ΔM_D stalling moment on airfoil plus flap, referred to quarter-chord point

ΔM_R hinge moment on flap, positive in same sense as ΔM_D

$\left(\frac{l}{2}\right)q_S$ downward displacement of quarter-chord point

q_D rotation of airfoil in stalling direction

q_R rotation of flap in stalling direction

$$\left.\begin{aligned}
k_{gh} &= k_{gh}' + ik_{gh}'' \\
q_h &= \left(q_h' + iq_h''\right)e^{i\omega t}
\end{aligned}\right\} \quad g, h = S, D, R$$

The quantities c_{gh} may be expressed in terms of the functions Φ_4, Φ_7, and Φ_{12} defined in reference 6 as follows:

c_{gh}

g \ h	S	D	R
S	1	1/2	$\Phi_4/2\pi$
D	1/2	3/8	$\Phi_7/4\pi$
R	$\Phi_4/2\pi$	$\Phi_7/4\pi$	$\Phi_{12}/4\pi^2$

DISCUSSION OF NUMERICAL RESULTS

The coefficients k_{SS}, k_{DS}, k_{SD}, and k_{DD}, which do not depend on the ratio of flap chord to total chord τ_R, are presented in table III and in figures 1 to 8 for $M = 0.7$ and a range of ω_r from 0 to 0.7.

The hinge-moment coefficients k_{RS} and k_{RD} associated with airfoil flapping and rotational motions are presented in table IV and figures 9 to 12 for $M = 0.7$, reduced frequencies from $\omega_r = 0$ to 0.7, and ratios $\tau_R = 0.15$, 0.24, 0.33, and 0.42. Coefficients P_n in the series representation for γ

$$\gamma \approx -2V\left(P_0 \cot \frac{\phi}{2} + 2 \sum_{n=1}^{4} P_n \sin n\phi\right)$$

are presented in table V for both flapping and rotational motions. It is noted that the coefficients k_{RS} and k_{RD} may be computed for any ratio of flap chord to total chord without further iterations by inserting the coefficients P_n for the appropriate type of airfoil motion into the formula

$$k_{Rh} = \left(c_{Rh}\omega_r^2 + \frac{1}{\pi}\sum_n P_n'Q_n\right) + i\left(\frac{1}{\pi}\sum_n P_n''Q_n\right), \quad h = S, D$$

The quantities Q_n are expressed as functions of τ_R as follows:

$$\cos\theta = 2\tau_R - 1, \quad 0 \leq \theta \leq \pi$$

$$Q_0 = (\pi - \theta)(-1 + 2\cos\theta) + 2\sin\theta - \frac{1}{2}\sin 2\theta$$

$$Q_1 = 2(\pi - \theta)\cos\theta + \frac{3}{2}\sin\theta + \frac{1}{6}\sin 3\theta$$

$$Q_2 = -(\pi - \theta) - \frac{2}{3}\sin 2\theta + \frac{1}{12}\sin 4\theta$$

$$Q_n = \frac{\sin(n-2)\theta}{(n-1)(n-2)} - \frac{2\sin n\theta}{(n-1)(n+1)} + \frac{\sin(n+2)\theta}{(n+1)(n+2)}, \quad n > 2$$

The aerodynamic coefficients associated with rotational motion of the flap k_{SR}, k_{DR}, and k_{RR} are presented in table VI and figures 13 to 18 for $M = 0.7$, reduced frequencies ranging from $\omega_r = 0$ to 0.7, and ratios of flap chord to total chord $\tau_R = 0.15$, 0.24, 0.33, and 0.42.

From five to eight iterations have been employed in the calculation of γ. In computing the coefficient k_{RR} the accuracy depends on the number of coefficients used as a starting basis for γ_{inc}. The number of coefficients is reduced by 3 in each successive iteration; in the calculations described in this report 22 coefficients have been used as a starting basis. All coefficients available at a given stage of the iteration have been used to calculate the contribution of γ_n to γ and the contribution of γ_{inc} has been obtained in closed form from the results of reference 6.

In recalculating the coefficients which are independent of τ_R and of the remaining coefficients for $\tau_R = 0.15$, values have been obtained which differ in general by less than 1 percent from those given by Dietze. There are a few isolated exceptions, however. An error of 7 percent has been found in the imaginary part of k_{DS} for $\omega_r = 0.10$. Also there are errors in Dietze's values of the imaginary part of k_{RS} at $\omega_r = 0.02$ for all Mach numbers tabulated, including $M = 0$. The entry for $M = 0$ should read $10^4 k_{RS}'' = 1.18$ instead of 1.03. Apparently the same error has been carried through for all Mach numbers. A similar error occurs in the imaginary part of k_{RD} at $\omega_r = 0.60$; the entry for $M = 0$ should be $10^4 k_{RD}'' = 131.8$ instead of 132.8, and this error has been carried through for other values of Mach number as well.

Chance Vought Aircraft
Division of United Aircraft Corporation
Dallas, Tex., July 19, 1949

REFERENCES

1. Possio, C.: L'Azione Aerodinamica sul Profilo Oscillante alle Velocità Ultrasonore. Acta, Pontificia Acad. Scientiarum, vol. I, n. 11, 1937, pp. 93-106.

2. Dietze, [F.]: Die Luftkräfte des harmonisch schwingenden Flügels im kompressiblen Medium bei Unterschallgeschwindigkeit (Ebenes Problem). Teil I: Berechnungsverfahren. Deutsche Luftfahrtforschung, Forschungsbericht Nr. 1733, Jan. 20, 1943. (Also available from CADO, Wright-Patterson Air Force Base, as AAF Translation No. F-TS-506-RE (ATI 6961), Nov. 1946.)

3. Dietze, [F.]: Die Luftkräfte des harmonisch schwingenden Flügels im kompressiblen Medium bei Unterschallgeschwindigkeit (Ebenes Problem). Teil II: Zahlen- und Kurventafeln. Deutsche Luftfahrtforschung, Forschungsbericht Nr. 1733/2, Jan. 24, 1944. (Also available from CADO, Wright-Patterson Air Force Base, as Translation No. F-TS-948-RE (ATI 9876), March 1947.)

4. Karp, S. N., and Weil, H.: The Oscillating Airfoil in Compressible Flow. Monograph III, Part II - A Review of Graphical and Numerical Data. Tech. Rep. No. F-TR-1195-ND, Air Materiel Command, U. S. Air Force, June 1948.

5. Karp, S. N., Shu, S. S., and Weil, H.: Monograph III - Aerodynamics of the Oscillating Airfoil in Compressible Flow. Tech. Rep. No. F-TR-1167-ND, Air Materiel Command, Army Air Forces, Oct. 1947.

6. Küssner, H. G., and Schwarz, L.: Der schwingende Flügel mit aerodynamisch ausgeglichenem Ruder. Luftfahrtforschung, Bd. 17, Nr. 11/12, Dec. 10, 1940, pp. 337-354. (Also available as NACA TM 991, 1941.)

7. Jahnke, E., and Emde, F.: Tables of Functions with Formulae and Curves. Dover Publications, 1943.

8. Watson, G. N.: A Treatise on the Theory of Bessel Functions. Second ed., The Macmillan Co., 1944.

9. Scarborough, James B.: Numerical Mathematical Analysis. The Johns Hopkins Press (Baltimore), 1930.

TABLE I.- VALUES OF α_i AND β_{ik} FOR M = 0.7

$\left[\alpha_i = \alpha_i' + i\alpha_i''; \quad \beta_{ik} = \beta_{ik}' + i\beta_{ik}''\right]$

ω_r	α_1		α_2		α_3	
	α_1'	α_1''	α_2'	α_2''	α_3'	α_3''
0.02	0	-0.04801	-0.00094	0	0	0.00001
.04	0	-.09601	-.00376	0	0	.00006
.06	0	-.14402	-.00847	0	0	.00021
.08	0	-.19202	-.01506	0	0	.00049
.10	0	-.24003	-.02353	0	0	.00095
.20	0	-.48006	-.09418	0	0	.00762
.30	0	-.72009	-.21179	0	0	.02573
.40	0	-.96012	-.37652	0	0	.06099
.50	0	-1.20015	-.58831	0	0	.11912
.60	0	-1.44018	-.84716	0	0	.20584
.70	0	-1.68021	-1.15308	0	0	.32686

ω_r	β_{00}		β_{01}	
	β_{00}'	β_{00}''	β_{01}'	β_{01}''
0.02	-1.82233	0.40415	-0.00347	0.00169
.04	-1.63609	.64055	-.01064	.00688
.06	-1.45768	.80639	-.01952	.01519
.08	-1.29103	.92767	-.02917	.02624
.10	-1.13670	1.01832	-.03904	.03961
.20	-.52194	1.23247	-.08348	.13074
.30	-.07794	1.27472	-.11434	.24736
.40	.27370	1.24893	-.13107	.38037
.50	.57113	1.18299	-.13419	.52669
.60	.83322	1.08608	-.12388	.68538
.70	1.06903	.96176	-.09990	.85624

TABLE I.- VALUES OF α_i AND β_{ik}

FOR M = 0.7 - Continued

ω_r	β_{02}		β_{10}	
	β_{02}'	β_{02}''	β_{10}'	β_{10}''
0.02	-0.00001	-0.00001	-0.00416	0.00148
.04	-.00004	-.00009	-.01401	.00591
.06	-.00018	-.00024	-.02809	.01331
.08	-.00042	-.00048	-.04561	.02366
.10	-.00079	-.00081	-.06601	.03696
.20	-.00519	-.00360	-.19879	.14786
.30	-.01438	-.00769	-.36140	.33268
.40	-.02896	-.01257	-.53416	.59143
.50	-.04790	-.01796	-.70335	.92411
.60	-.07225	-.02363	-.85837	1.33071
.70	-.10161	-.02952	-.99061	1.81125

ω_r	β_{11}		β_{12}	
	β_{11}'	β_{11}''	β_{12}'	β_{12}''
0.02	-0.00001	-0.04802	0.00047	0
.04	-.00005	-.09611	.00188	0
.06	-.00016	-.14430	.00424	0
.08	-.00038	-.19262	.00753	0
.10	-.00075	-.24108	.01177	0
.20	-.00599	-.48583	.04706	0
.30	-.02020	-.73434	.10590	0
.40	-.04790	-.98513	.18826	0
.50	-.09356	-1.23571	.29416	0
.60	-.16166	-1.48287	.42358	0
.70	-.25672	-1.72280	.57654	0

TABLE I.- VALUES OF α_i AND β_{ik}

FOR M = 0.7 - Concluded

ω_r	β_{13}		β_{20}	
	β_{13}'	β_{13}''	β_{20}'	β_{20}''
0.02	0	-0.000004	0.000003	0.00001
.04	0	-.00003	.00002	.00005
.06	0	-.00010	.00008	.00014
.08	0	-.00024	.00019	.00030
.10	0	-.00048	.00037	.00053
.20	0	-.00381	.00299	.00288
.30	0	-.01286	.01010	.00713
.40	0	-.03049	.02395	.01251
.50	0	-.05956	.04678	.01778
.60	0	-.10292	.08083	.02134
.70	0	-.16343	.12836	.02130

ω_r	β_{21}		β_{22}		β_{23}	
	β_{21}'	β_{21}''	β_{22}'	β_{22}''	β_{23}'	β_{23}''
0.02	0	-0.04801	-0.00094	0	0	-0.000002
.04	0	-.09602	-.00376	0	0	-.00002
.06	0	-.14404	-.00847	0	0	-.00005
.08	0	-.19208	-.01506	0	0	-.00012
.10	0	-.24015	-.02353	0	0	-.00024
.20	0	-.48101	-.09413	0	0	-.00191
.30	0	-.72331	-.21179	0	0	-.00643
.40	0	-.96774	-.37652	0	0	-.01525
.50	0	-1.21504	-.58831	0	0	-.02978
.60	0	-1.46591	-.84716	0	0	-.05146
.70	0	-1.72106	-1.15308	0	0	-.08171

TABLE II.- VALUES OF KERNEL AND KERNEL DIFFERENCE

s	K'(s,0.7)	K''(s,0.7)	K'(s,0)	K''(s,0)	$\Delta K'(s,0.7)$	$\Delta K''(s,0.7)$	$\Delta K_1'(s,0.7)$	$\Delta K_1''(s,0.7)$	$\Delta K_2'(s,0.7)$	$\Delta K_2''(s,0.7)$
-2.040000	0.011560	0.012424	0.015418	-0.022375	-0.003858	0.034799	-0.077960	0.170551	0.074101	-0.135752
-1.748571	.001205	.021261	.021173	-.027647	-.019968	.048909	-.099707	.140884	.079739	-.091975
-1.457143	-.016623	.022300	.030307	-.035040	-.046930	.057339	-.120836	.109422	.073896	-.052083
-1.238571	-.032406	.013815	.041122	-.042762	-.073528	.056578	-.136632	.084184	.063105	-.027606
-1.020000	-.047369	-.007936	.058209	-.053466	-.105577	.045530	-.153120	.056930	.047542	-.011400
-.801429	-.051371	-.040850	.087487	-.069077	-.138858	.028227	-.171854	.026681	.032996	.001546
-.582857	-.034254	-.096274	.144397	-.093655	-.178651	-.002619	-.197094	-.008492	.018443	.005873
-.437143	.006705	-.150654	.220011	-.119616	-.213307	-.031038	-.223823	-.036742	.010516	.005704
-.291429	.112041	-.230339	.381832	-.161756	-.269791	-.068583	-.274424	-.072497	.004632	.003913
-.218571	.228886	-.288192	.550946	-.195116	-.322060	-.093076	-.324627	-.095786	.002566	.002710
-.145714	.474420	-.371253	.899102	-.246179	-.424681	-.125074	-.425794	-.126578	.001113	.001504
-.072857	1.237186	-.516904	1.970378	-.341703	-.733192	-.175201	-.733459	-.175698	.000267	.000497
-.043714	2.268691	-.626625	3.415745	-.416610	-1.147054	-.210016	-1.147150	-.210226	.000096	.000210
.043714	-2.968175	-.610725	-3.915267	-.394760	.947092	-.215966	.947010	-.216180	.000082	.000214
.072857	-1.935504	-.490413	-2.469051	-.305307	.533547	-.185106	.533319	-.185622	.000228	.000516
.145714	-1.167286	-.318355	-1.393803	-.173580	.226517	-.144775	.225654	-.146425	.000862	.001650
.218571	-.912709	-.209057	-1.039050	-.086699	.126341	-.122358	.124487	-.125556	.001854	.003197
.291429	-.783300	-.125224	-.860749	-.018096	.077449	-.107128	.074284	-.112190	.003165	.005062
.437143	-.642669	.005298	-.672994	.092060	.030324	-.086762	.023683	-.096282	.006642	.009520
.582857	-.553769	.108392	-.561844	.181551	.008075	-.073158	-.003046	-.087878	.011121	.014720
.801429	-.444153	.231165	-.435327	.290098	-.008826	-.058933	-.028286	-.082475	.019460	.023542
1.020000	-.336260	.321970	-.319892	.372588	-.016369	-.050618	-.047020	-.081996	.030652	.031379
1.238571	-.226728	.389086	-.204195	.429897	-.022532	-.040811	-.063508	-.084512	.040975	.043702
1.457143	-.112563	.427351	-.087011	.461734	-.025552	-.034383	-.079314	-.089044	.053762	.054660
1.748571	.039420	.437118	.067247	.464472	-.027827	-.027354	-.100433	-.097275	.072605	.069921
2.040000	.181763	.402045	.210670	.423589	-.028906	-.021544	-.122180	-.107301	.093274	.085757

TABLE III.- AERODYNAMIC COEFFICIENTS, INDEPENDENT OF RATIO OF FLAP CHORD TO TOTAL CHORD

[M = 0.7]

Coefficient \ ω_r	0	0.02	0.04	0.06	0.08	0.1	0.2	0.3	0.4	0.5	0.6	0.7
$k_{SS}' \times 10^4$	0	75.0	216.2	373.8	534.6	688.6	1347	1893	2432	3034	3798	4767
$k_{SS}'' \times 10^4$	0	517.0	952.4	1323	1650	1944	3188	4334	5530	6838	8252	9789
$k_{DS}' \times 10^4$	0	-3.0	-11.4	-23.5	-38.6	-56.1	-173.3	-337.4	-546.2	-791.2	-1010	-1173
$k_{DS}'' \times 10^4$	0	0.5	3.4	8.2	16.3	26.9	115.3	271.8	522.2	904.7	1459	2222
$k_{SD}' \times 10^4$	28,006	25,937	24,025	22,430	21,191	20,186	17,461	16,676	16,802	17,487	18,569	19,909
$k_{SD}'' \times 10^4$	0	-3046	-4058	-4323	-4253	-3969	-1659	750.5	2929	4851	6468	7757
$k_{DD}' \times 10^4$	0	25.5	72.8	125.6	179.1	236.9	508.9	838.0	1301	1972	2883	4136
$k_{DD}'' \times 10^4$	0	399.4	770.9	1122	1460	1792	3402	5044	6760	8532	10,302	11,973

TABLE IV.- HINGE-MOMENT COEFFICIENTS FOR FLAPPING AND ROTATION OF AIRFOIL

Coefficient	ω_r / τ_R	0	0.02	0.04	0.06	0.08	0.1	0.2	0.3	0.4	0.5	0.6	0.7
$k_{RS}' \times 10^4$	0.15	0	0.2	0.5	0.7	1.0	1.2	1.0	-0.6	-3.6	-7.9	-13.0	-19.1
$k_{RS}'' \times 10^4$		0	1.6	3.0	4.2	5.3	6.3	11.2	16.2	21.9	28.8	37.7	49.1
$k_{RS}' \times 10^4$	0.24	0	0.6	1.6	2.5	3.4	4.1	3.9	-0.6	-9.4	-22.2	-36.9	-53.9
$k_{RS}'' \times 10^4$		0	5.3	9.8	13.8	17.4	20.8	36.9	53.6	73.0	97.0	127.7	167.9
$k_{RS}' \times 10^4$	0.33	0	1.4	3.7	6.0	7.9	9.6	10.5	1.8	-15.4	-40.9	-69.0	-100.3
$k_{RS}'' \times 10^4$		0	11.9	22.2	31.2	39.5	47.2	83.5	121.7	166.7	222.8	295.0	389.4
$k_{RS}' \times 10^4$	0.42	0	2.6	7.1	11.5	15.4	18.6	22.5	9.6	-17.7	-58.2	-100.8	-145.2
$k_{RS}'' \times 10^4$		0	22.4	41.6	58.5	74.0	88.4	156.0	227.7	313.0	420.2	558.3	738.2
$k_{RD}' \times 10^4$	0.15	85.7	79.7	74.5	70.2	67.0	64.4	57.0	54.0	53.1	53.8	57.3	64.2
$k_{RD}'' \times 10^4$		0	-2.6	0.5	5.7	11.6	18.1	52.8	88.5	125.2	163.2	200.8	240.9
$k_{RD}' \times 10^4$	0.24	283.7	263.8	246.5	232.4	221.6	213.2	189.9	182.4	183.4	191.5	209.1	239.8
$k_{RD}'' \times 10^4$		0	-10.0	-0.7	15.1	33.6	54.1	163.4	276.5	392.9	513.3	633.5	760.0
$k_{RD}' \times 10^4$	0.33	644.0	598.9	559.3	527.1	502.8	483.8	433.2	421.3	431.0	460.4	512.3	597.2
$k_{RD}'' \times 10^4$		0	-25.6	-7.4	25.9	65.3	109.3	345.1	589.2	840.5	1100	1360	1631
$k_{RD}' \times 10^4$	0.42	1207	1122	1048	987.4	941.7	906.3	815.0	800.6	830.8	903.0	1019	1200
$k_{RD}'' \times 10^4$		0	-53.6	-24.8	32.5	101.5	179.1	597.3	1031	1476	1935	2365	2863

TABLE V.- VALUES OF COEFFICIENTS P_n IN SERIES REPRESENTATION

$$\gamma = -2V\left(P_0 \cot\frac{\phi}{2} + 2\sum_n P_n \sin n\phi\right)$$

$$\left[P_n = P_n' + iP_n''\right]$$

For flapping of airfoil						
	$\omega_r = 0.02$		$\omega_r = 0.04$		$\omega_r = 0.06$	
n	P_n'	P_n''	P_n'	P_n''	P_n'	P_n''
0	0.00405	0.02580	0.01195	0.04726	0.02102	0.06523
1	-.00050	.00005	-.00194	.00036	-.000413	.00091
2	0	0	0	.00003	.00002	.00009
3	0	0	0	0	0	0
4	0	0	0	0	0	0

	$\omega_r = 0.08$		$\omega_r = 0.10$		$\omega_r = 0.20$		$\omega_r = 0.30$	
n	P_n'	P_n''	P_n'	P_n''	P_n'	P_n''	P_n'	P_n''
0	0.03053	0.08067	0.03991	0.09420	0.08342	0.14570	0.12386	0.18312
1	-.00700	.00181	-.01048	.00302	-.03610	.01371	-.07419	.03356
2	.00006	.00018	.00013	.00034	.00123	.00218	.00454	.00039
3	0	0	.00011	-.00004	.00013	-.00007	.00057	-.00043
4	0	0	0	0	0	0	-.00004	-.00003

	$\omega_r = 0.40$		$\omega_r = 0.50$		$\omega_r = 0.60$		$\omega_r = 0.70$	
n	P_n'	P_n''	P_n'	P_n''	P_n'	P_n''	P_n'	P_n''
0	0.16431	0.21075	0.20492	0.22786	0.24175	0.23334	0.27133	0.22743
1	-.12273	.06574	-.17824	.11402	-.23186	.17927	-.27797	.26203
2	.01189	.01353	.02588	.02355	.04912	.03341	.08434	.03984
3	.00167	-.00157	.00378	-.00432	.00634	-.01014	.00848	-.02027
4	-.00018	-.00014	-.00059	-.00044	-.00165	-.00096	-.00355	-.00157

TABLE V.- VALUES OF COEFFICIENTS P_n IN SERIES REPRESENTATION

$$\gamma = -2V\left(P_0 \cot \frac{\phi}{2} + 2 \sum_n P_n \sin n\phi\right)$$ - Concluded

For rotation of airfoil						
	$\omega_r = 0.02$		$\omega_r = 0.04$		$\omega_r = 0.06$	
n	P_n'	P_n''	P_n'	P_n''	P_n'	P_n''
0	1.29401	-0.19220	1.19290	-0.27984	1.10671	-0.32806
1	.00272	.03991	.00793	.07696	.01391	.11189
2	.00032	-.00003	.00125	-.00013	.00270	-.00035
3	0	0	0	0	0	0
4	0	0	0	0	0	0

	$\omega_r = 0.08$		$\omega_r = 0.10$		$\omega_r = 0.20$		$\omega_r = 0.30$	
n	P_n'	P_n''	P_n'	P_n''	P_n'	P_n''	P_n'	P_n''
0	1.03781	-0.35794	0.97989	-0.37637	0.80131	-0.41701	0.70475	-0.45044
1	.02012	.14529	.02691	.17790	.06175	.33405	.10655	.48796
2	.00461	-.00069	.00697	-.00126	.02586	-.00612	.05649	-.01645
3	0	-.00009	-.00004	-.00018	-.00037	-.00135	-.00159	-.00454
4	0	0	0	0	-.00004	0	-.00029	.00014

	$\omega_r = 0.40$		$\omega_r = 0.50$		$\omega_r = 0.60$		$\omega_r = 0.70$	
n	P_n'	P_n''	P_n'	P_n''	P_n'	P_n''	P_n'	P_n''
0	0.63101	-0.49399	0.55644	-0.54194	0.47233	-0.59052	0.37484	-0.61770
1	.16912	.64043	.25543	.78449	.36613	.91393	.49812	1.00553
2	.09907	-.03557	.15194	-.06873	.21279	-.11630	.26823	-.19176
3	-.00472	-.01080	-.01190	-.02105	-.02383	-.03601	-.04688	-.05153
4	-.00097	.00055	-.00196	-.00169	.00531	.00378	-.00929	.00848

TABLE VI.- AERODYNAMIC COEFFICIENTS DUE TO FLAP ROTATION

[M = 0.7]

Coefficient	ω_r / τ_R	0	0.02	0.04	0.06	0.08	0.1	0.2	0.3	0.4	0.5	0.6	0.7
$k_{SR}' \times 10^4$	0.15	13,458	12,411	11,392	10,524	9801	9194	7320	6373	5780	5319	4901	4475
$k_{SR}'' \times 10^4$		0	-1858	-2690	-3123	-3350	-3459	-3402	-3187	-3042	-2961	-2917	-2869
$k_{SR}' \times 10^4$	0.24	16,742	15,321	14,206	13,145	12,267	11,538	9313	8296	7716	7314	6963	6628
$k_{SR}'' \times 10^4$		0	-2235	-3209	-3697	-3930	-4023	-3769	-3336	-3051	-2889	-2806	-2776
$k_{SR}' \times 10^4$	0.33	19,294	17,816	16,403	15,208	14,218	13,409	10,978	9928	9443	9164	8980	8824
$k_{SR}'' \times 10^4$		0	-2497	-3542	-4043	-4258	-4316	-3813	-3157	-2654	-2337	-2163	-2084
$k_{SR}' \times 10^4$	0.42	21,370	19,745	18,205	16,918	15,846	14,979	12,444	11,408	11,012	10,909	10,945	11,020
$k_{SR}'' \times 10^4$		0	-2674	-3753	-4229	-4417	-4425	-3684	-2723	-1984	-1446	-1116	-965.6
$k_{DR}' \times 10^4$	0.15	5411	5425	5453	5487	5522	5559	5738	5912	6074	6202	6280	6277
$k_{DR}'' \times 10^4$		0	63.4	111.9	148.3	176.0	194.9	225.2	177.5	59.6	-122.2	-364.6	-653.1
$k_{DR}' \times 10^4$	0.24	5787	5802	5836	5878	5922	5967	6204	6466	6768	7069	7342	7588
$k_{DR}'' \times 10^4$		0	122.2	225.5	315.1	393.2	463.4	735.5	949.4	1049	1063	980.5	809.9
$k_{DR}' \times 10^4$	0.33	5617	5634	5673	5721	5767	5823	6100	6415	6838	7284	7769	8262
$k_{DR}'' \times 10^4$		0	181.9	342.4	487.5	620.1	744.0	1284	1764	2160	2453	2633	2686
$k_{DR}' \times 10^4$	0.42	5104	5123	5166	5206	5271	5332	5640	6009	6466	7039	7702	8447
$k_{DR}'' \times 10^4$		0	237.6	452.9	650.3	836.5	1013	1819	2562	3273	3872	4375	4722
$k_{RR}' \times 10^4$	0.15	181.7	178.7	176.1	174.0	172.4	171.1	168.4	168.8	170.7	173.2	176.0	178.9
$k_{RR}'' \times 10^4$		0	-2.1	-1.4	0.4	2.7	5.1	19.0	32.1	44.3	55.9	66.2	75.8
$k_{RR}' \times 10^4$	0.24	482.3	470.8	460.1	451.3	444.6	438.5	427.7	429.5	438.9	452.0	467.5	484.2
$k_{RR}'' \times 10^4$		0	-9.0	-6.2	0.9	10.0	20.1	75.0	130.4	181.6	228.6	272.5	312.7
$k_{RR}' \times 10^4$	0.33	950.4	919.6	891.1	868.4	850.5	836.7	805.3	808.9	836.3	872.5	919.6	974.5
$k_{RR}'' \times 10^4$		0	-24.2	-17.5	0.2	23.2	49.0	189.2	329.8	466.1	591.9	708.3	817.1
$k_{RR}' \times 10^4$	0.42	1608	1543	1485	1436	1401	1373	1311	1319	1367	1448	1553	1684
$k_{RR}'' \times 10^4$		0	-51.7	-39.1	-4.1	42.1	94.3	376.1	662.2	942.2	1206	1444	1690

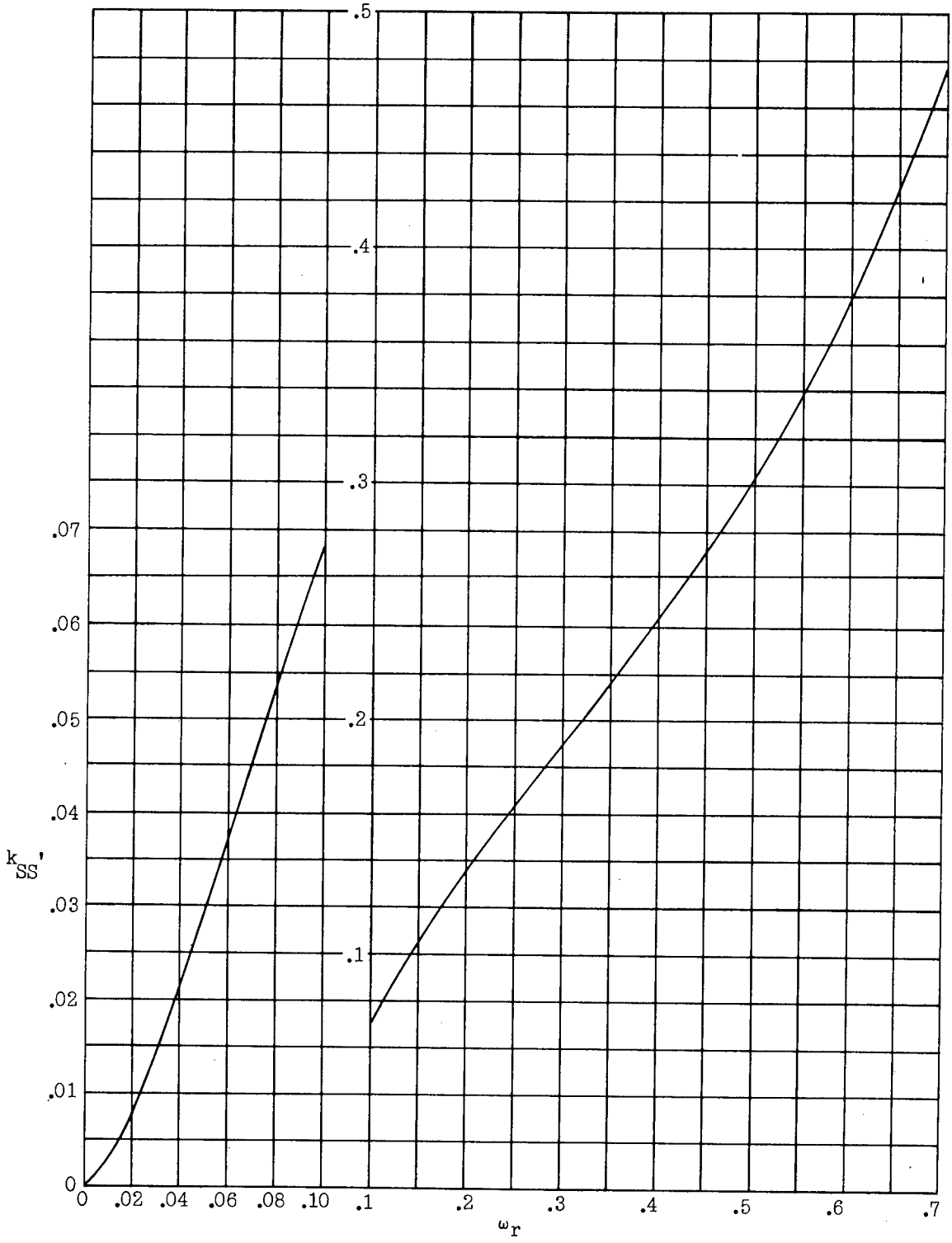

Figure 1.- Real part of k_{SS} against reduced frequency for $M = 0.7$.

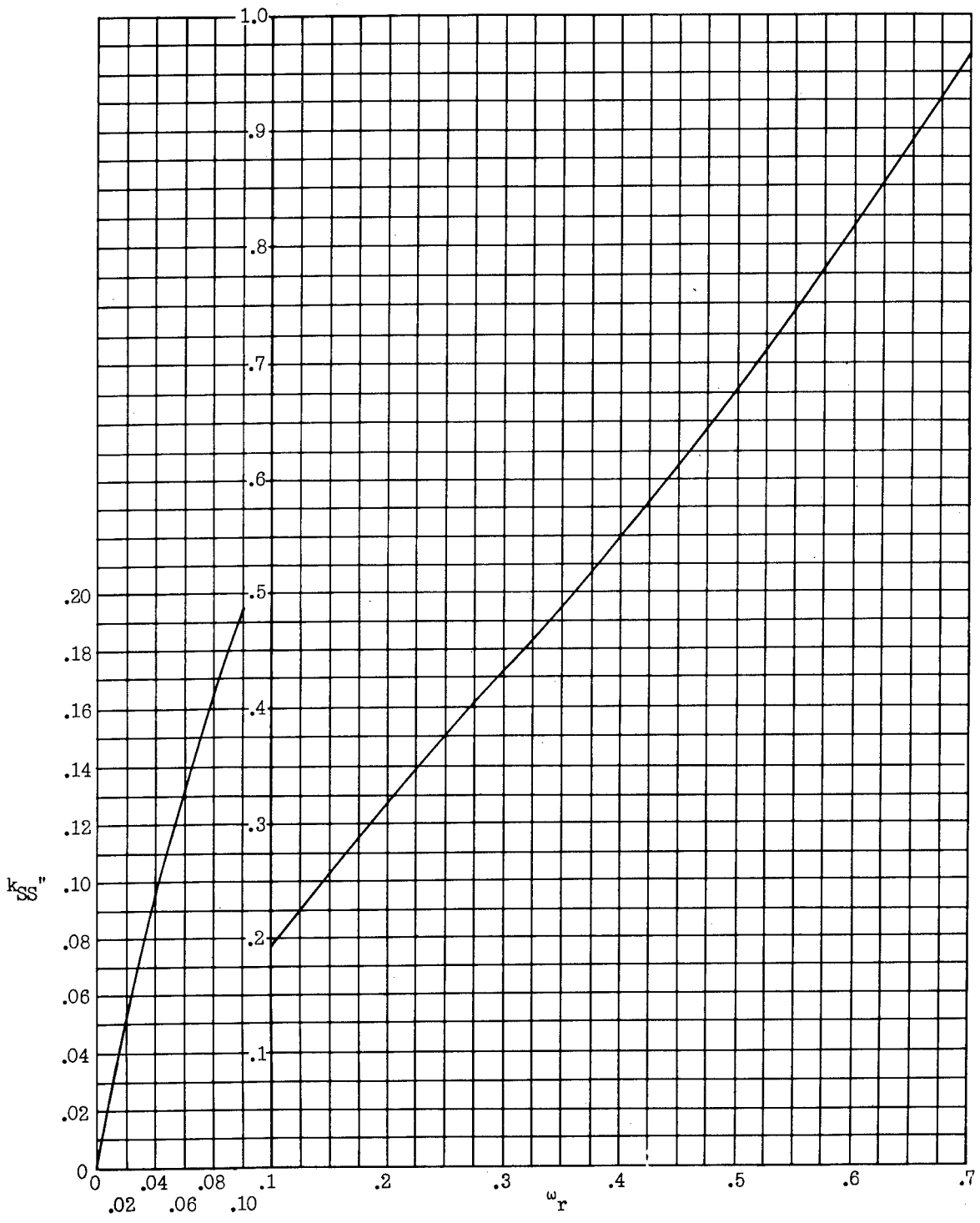

Figure 2.- Imaginary part of k_{SS} for M = 0.7.

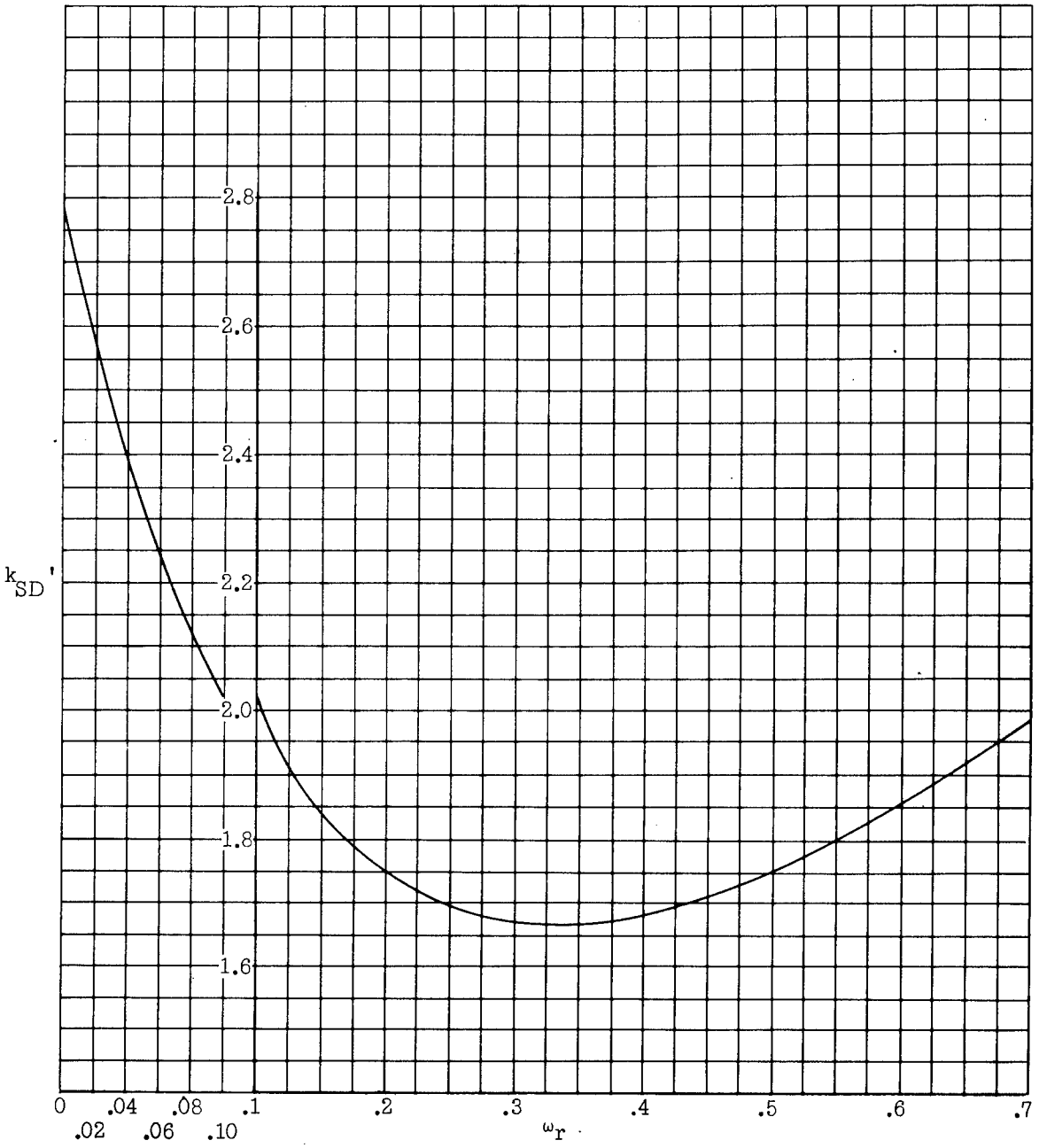

Figure 3.- Real part of k_{SD} for M = 0.7.

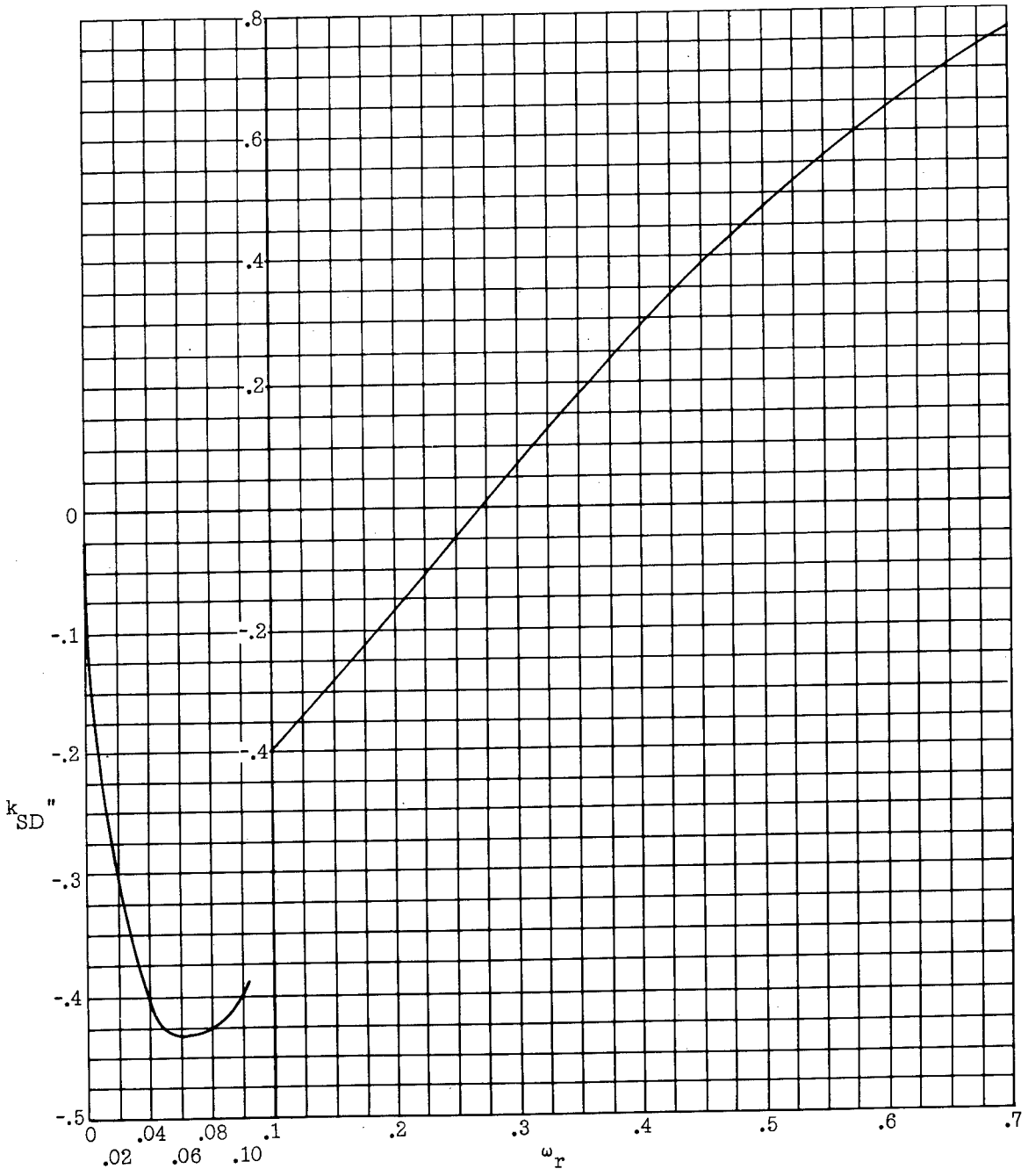

Figure 4.- Imaginary part of k_{SD} for M = 0.7.

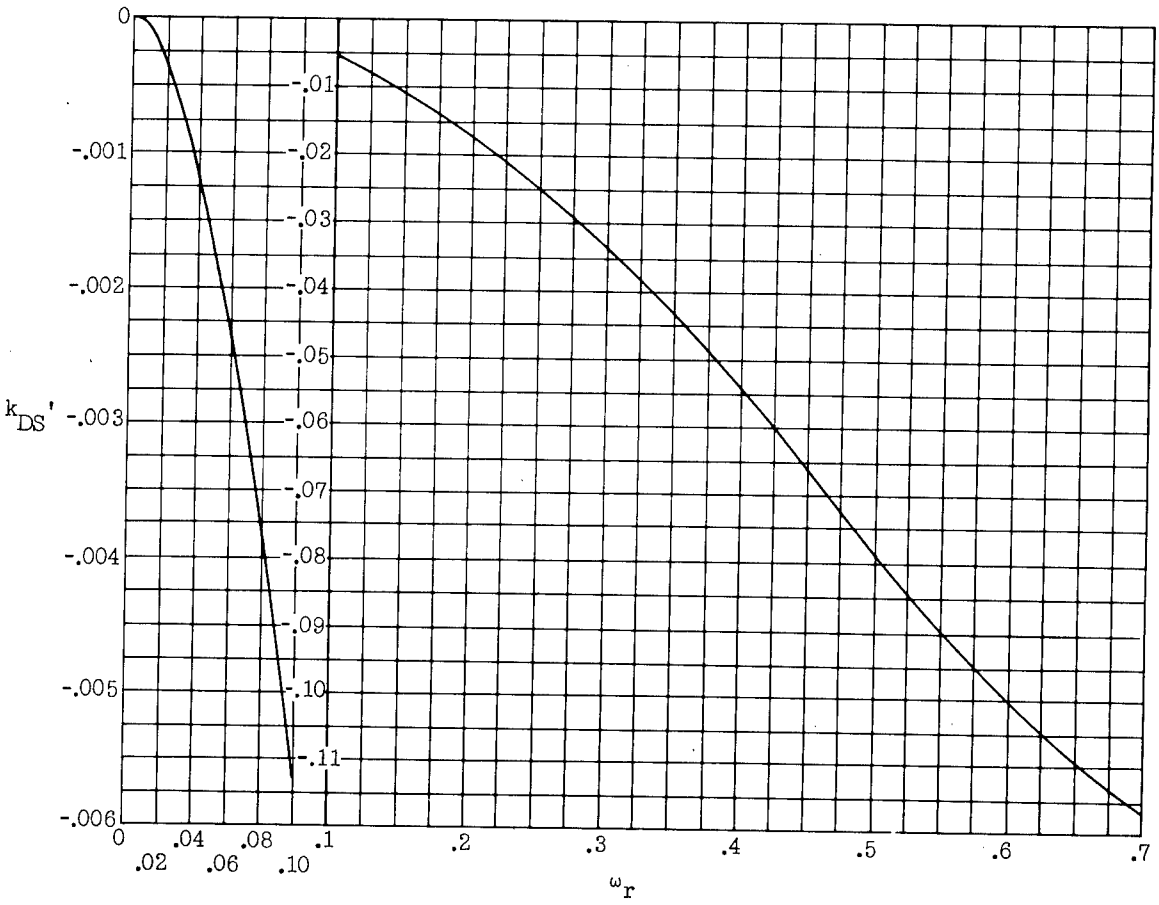

Figure 5.- Real part of k_{DS} for M = 0.7.

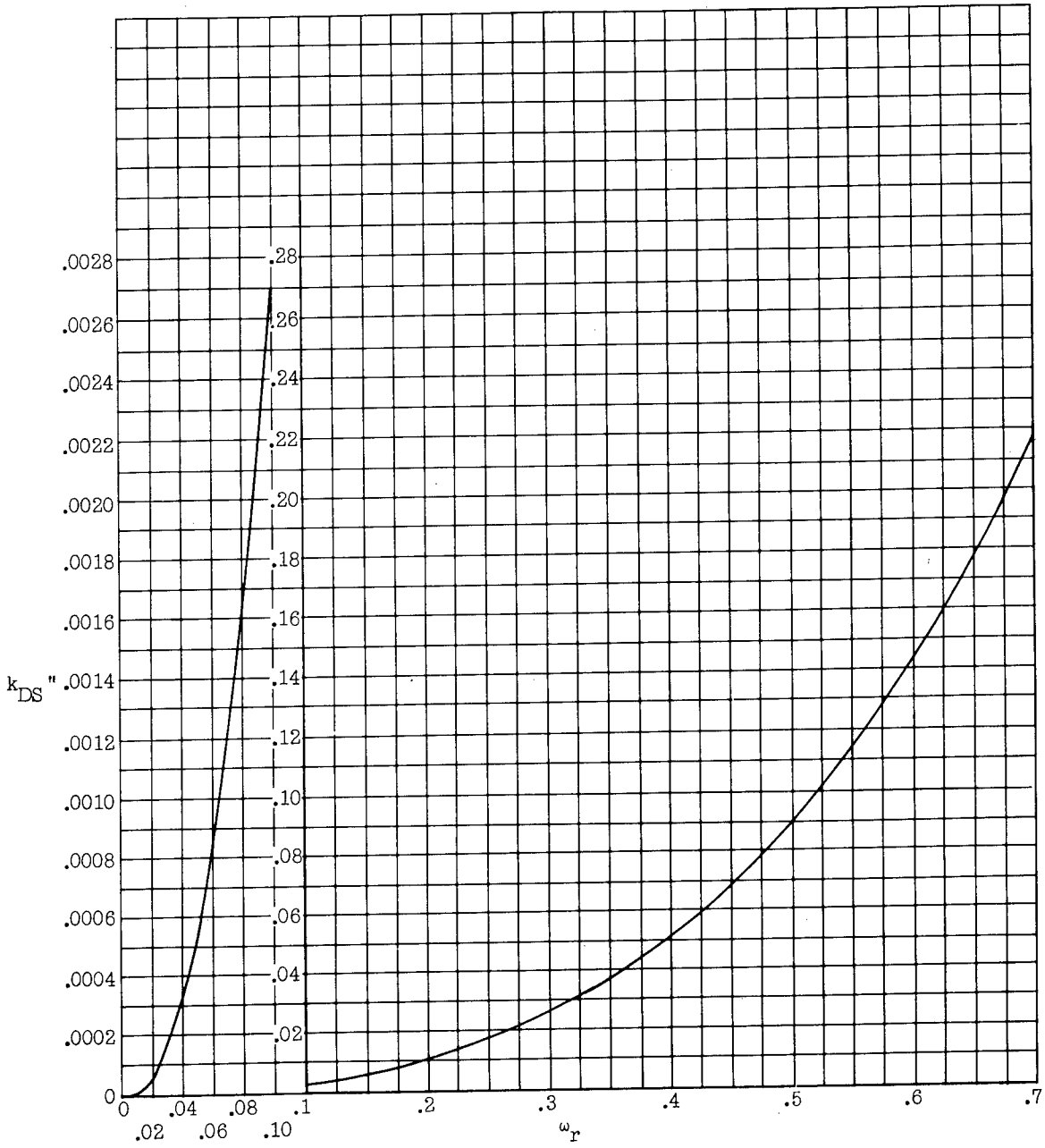

Figure 6.- Imaginary part of k_{DS} for M = 0.7.

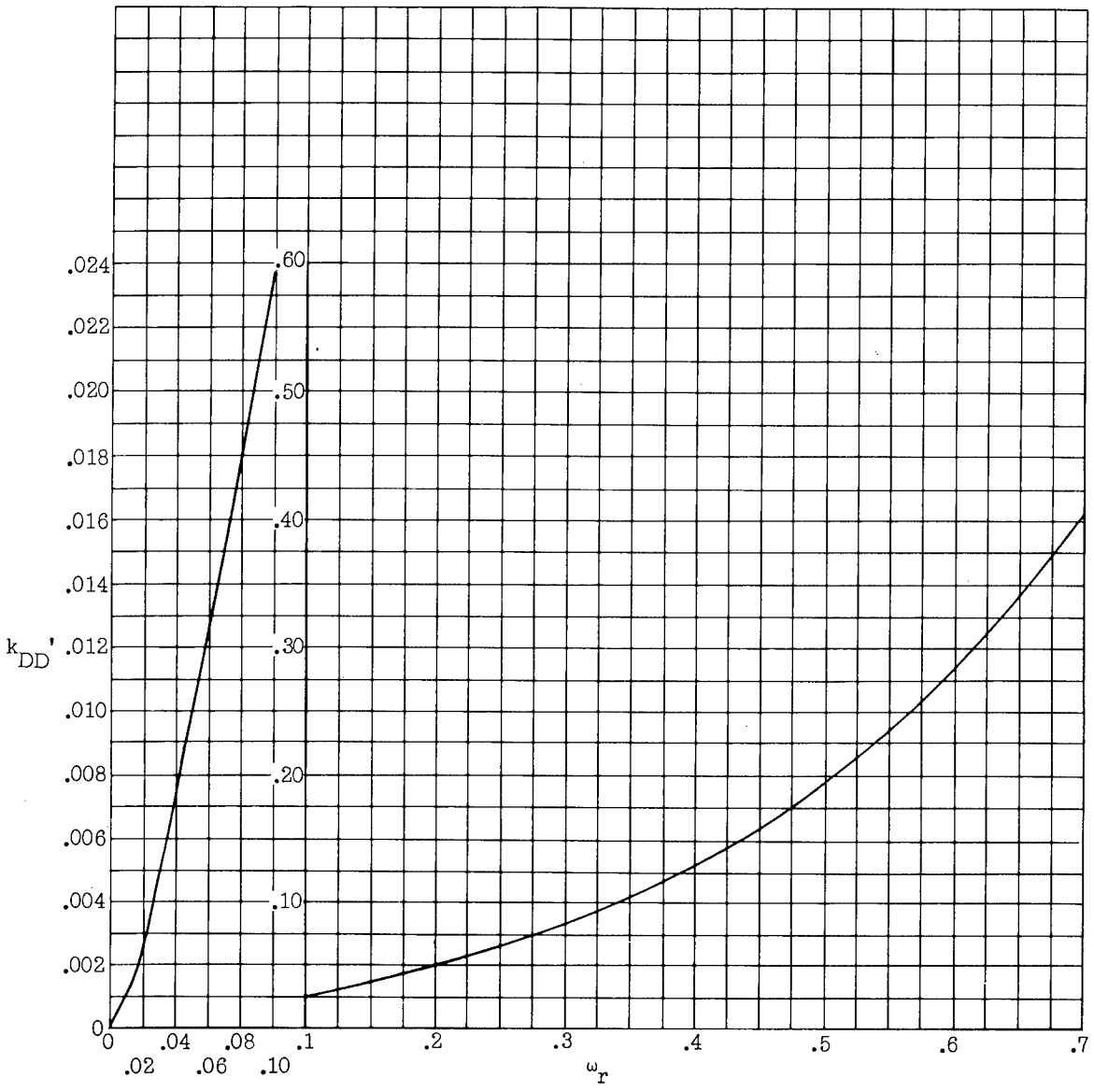

Figure 7.- Real part of k_{DD} for M = 0.7.

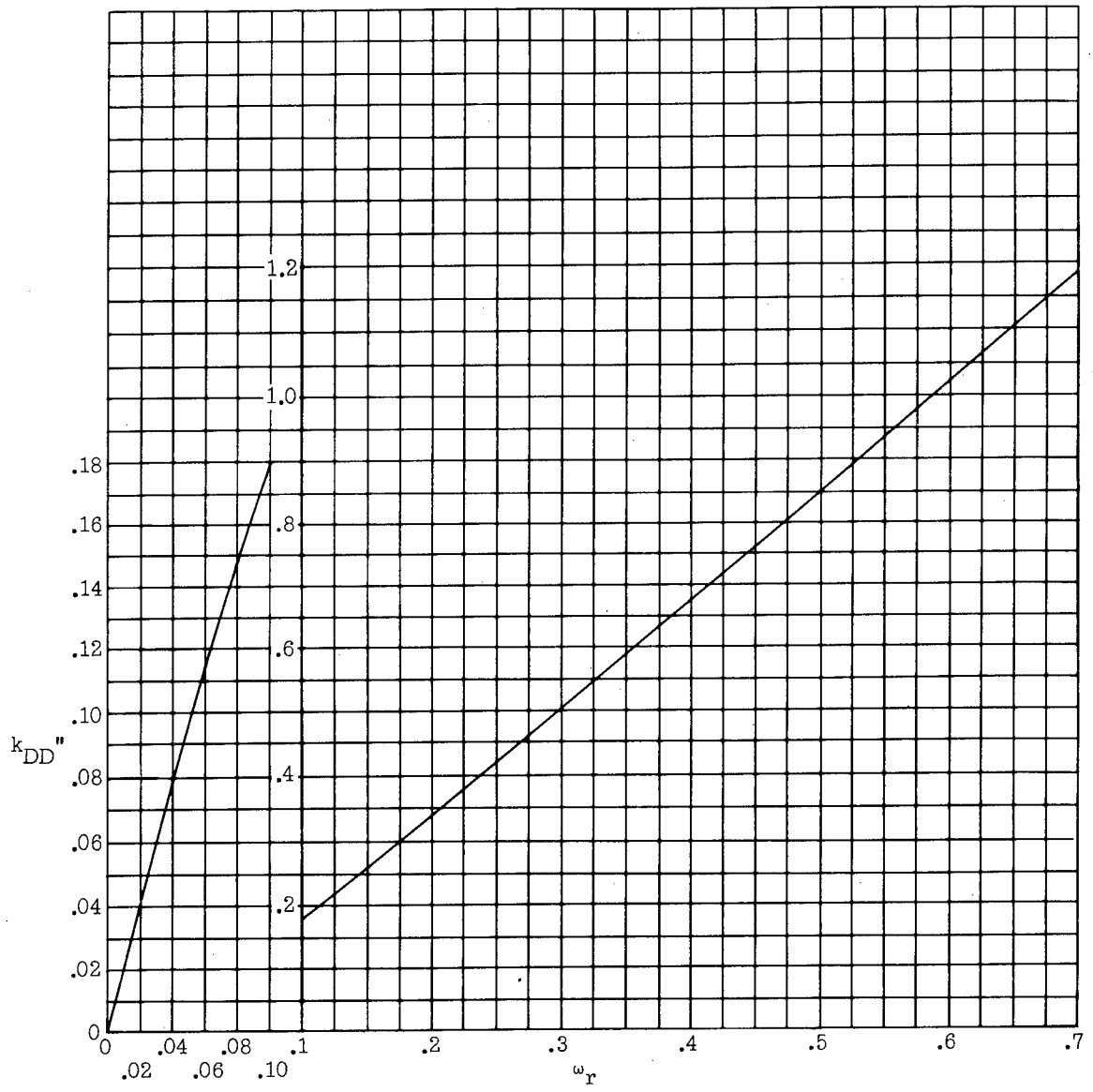

Figure 8.- Imaginary part of k_{DD} for M = 0.7.

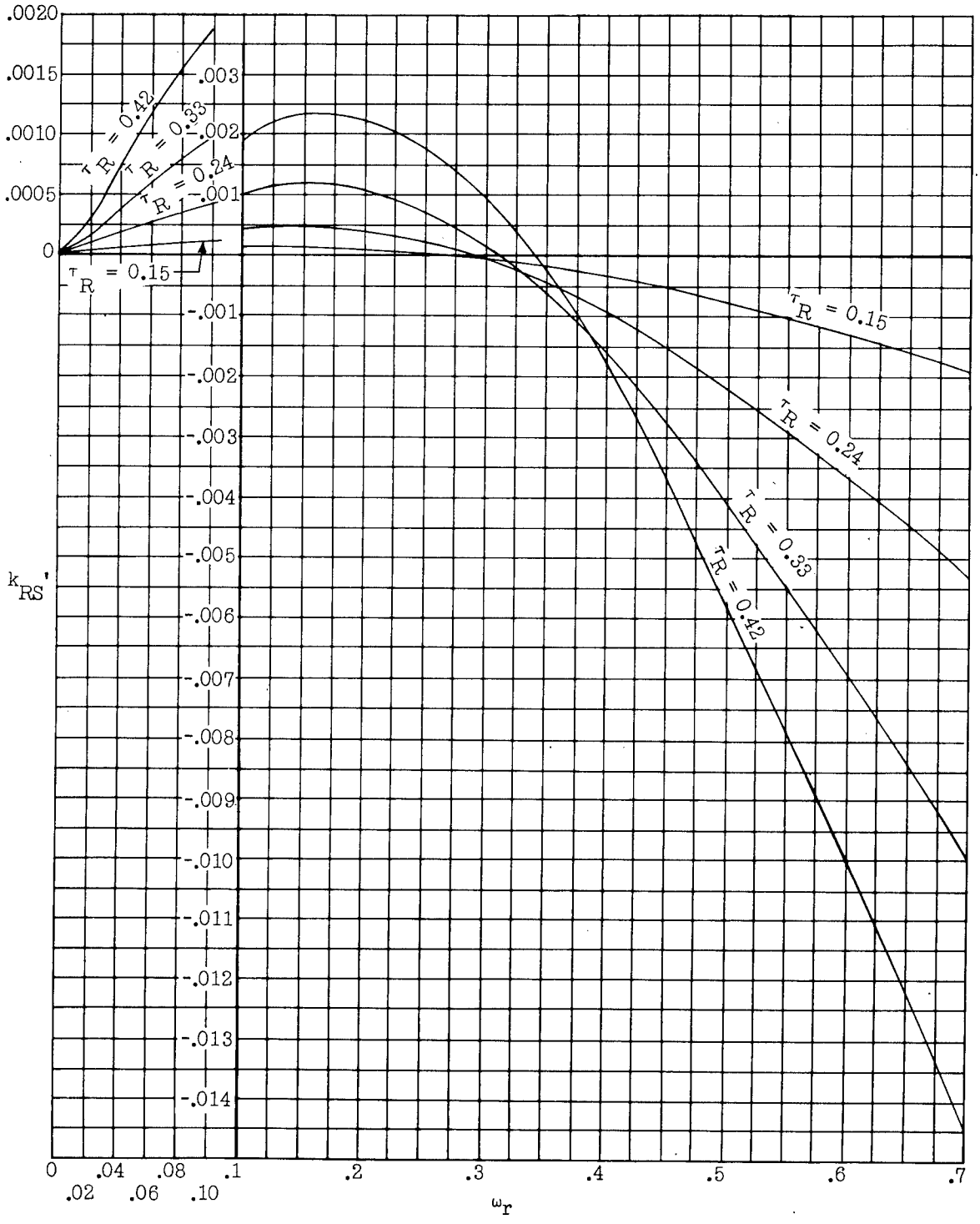

Figure 9.- Real part of k_{RS} for M = 0.7.

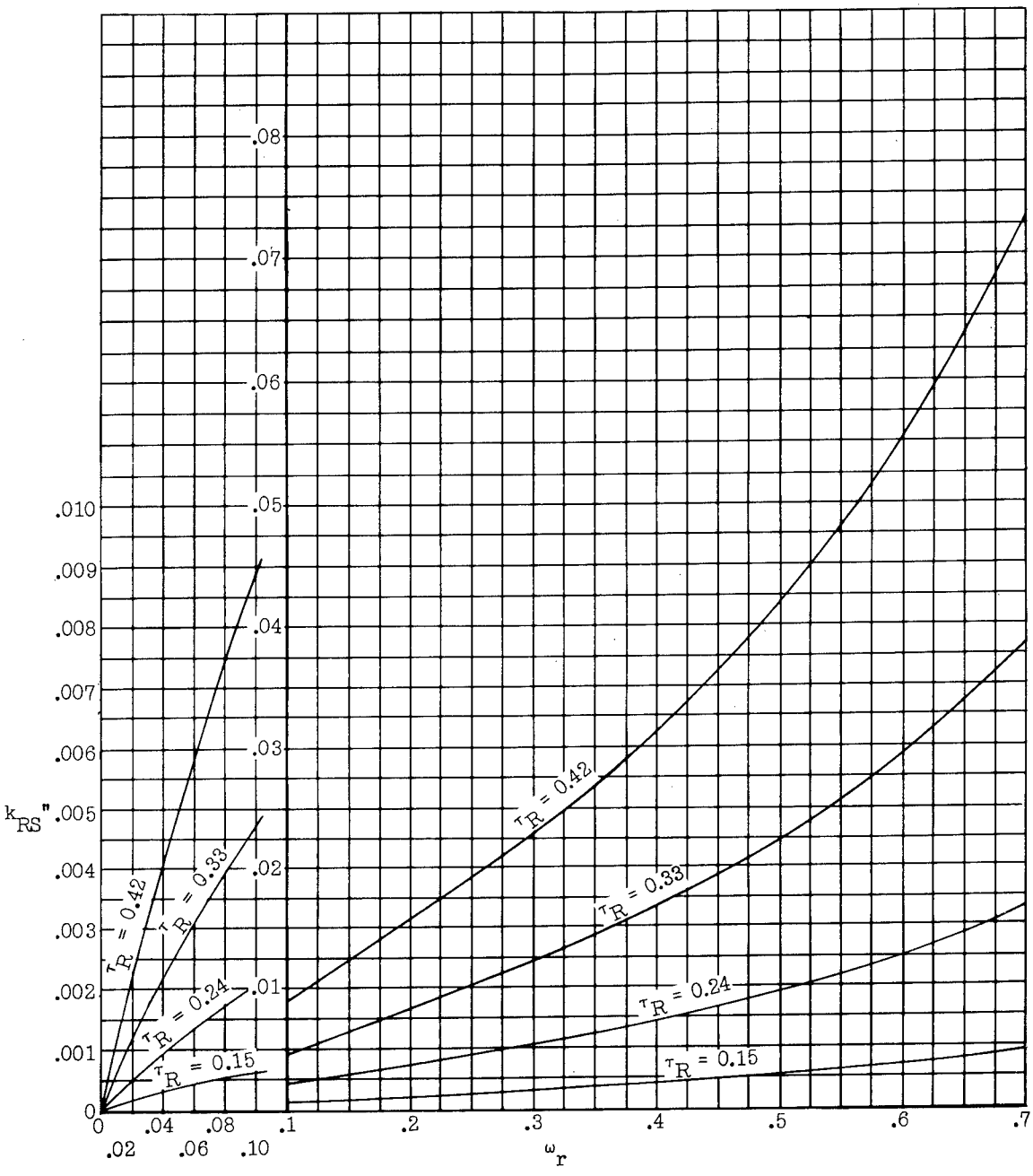

Figure 10.- Imaginary part of k_{RS} for M = 0.7.

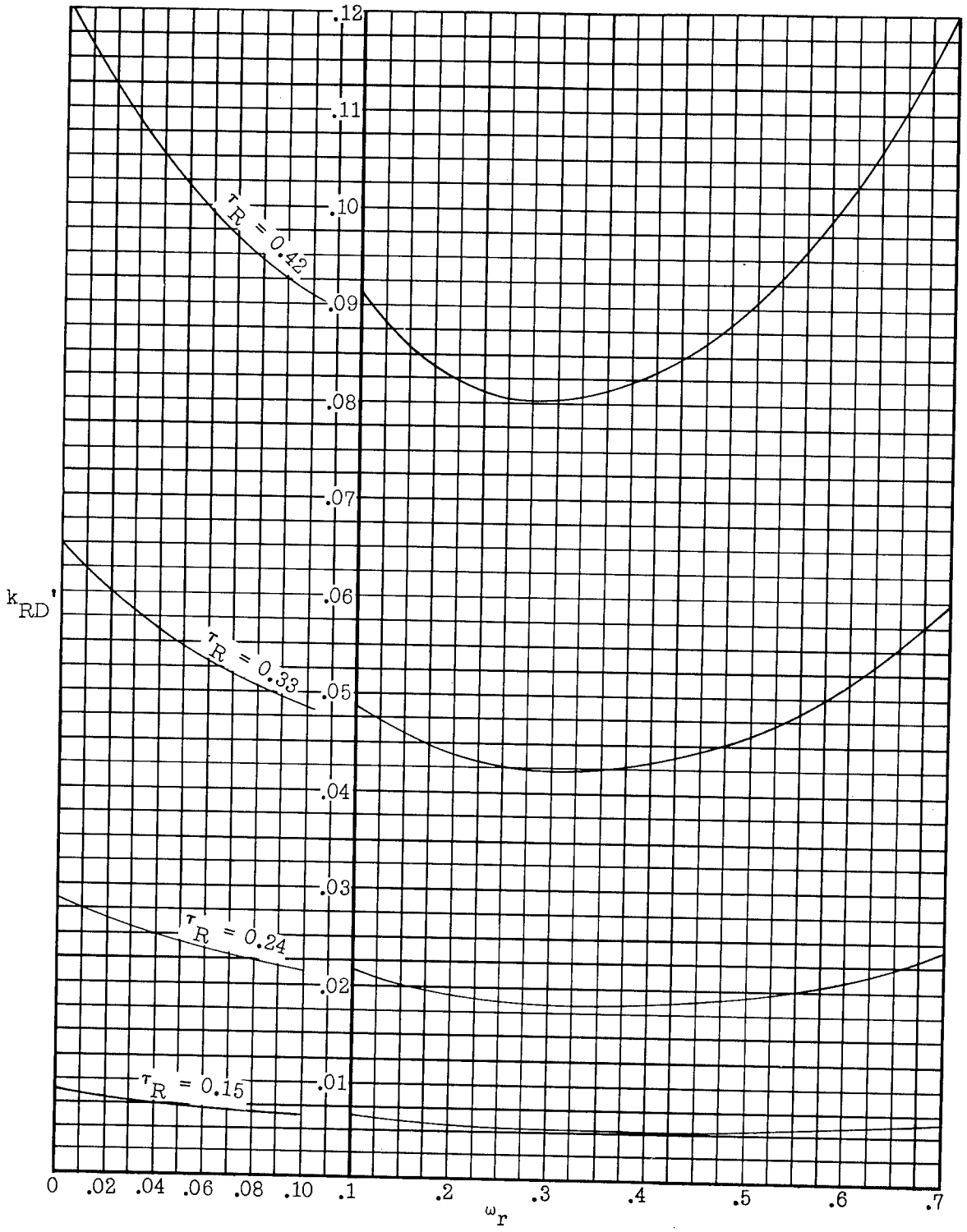

Figure 11.- Real part of k_{RD} for M = 0.7.

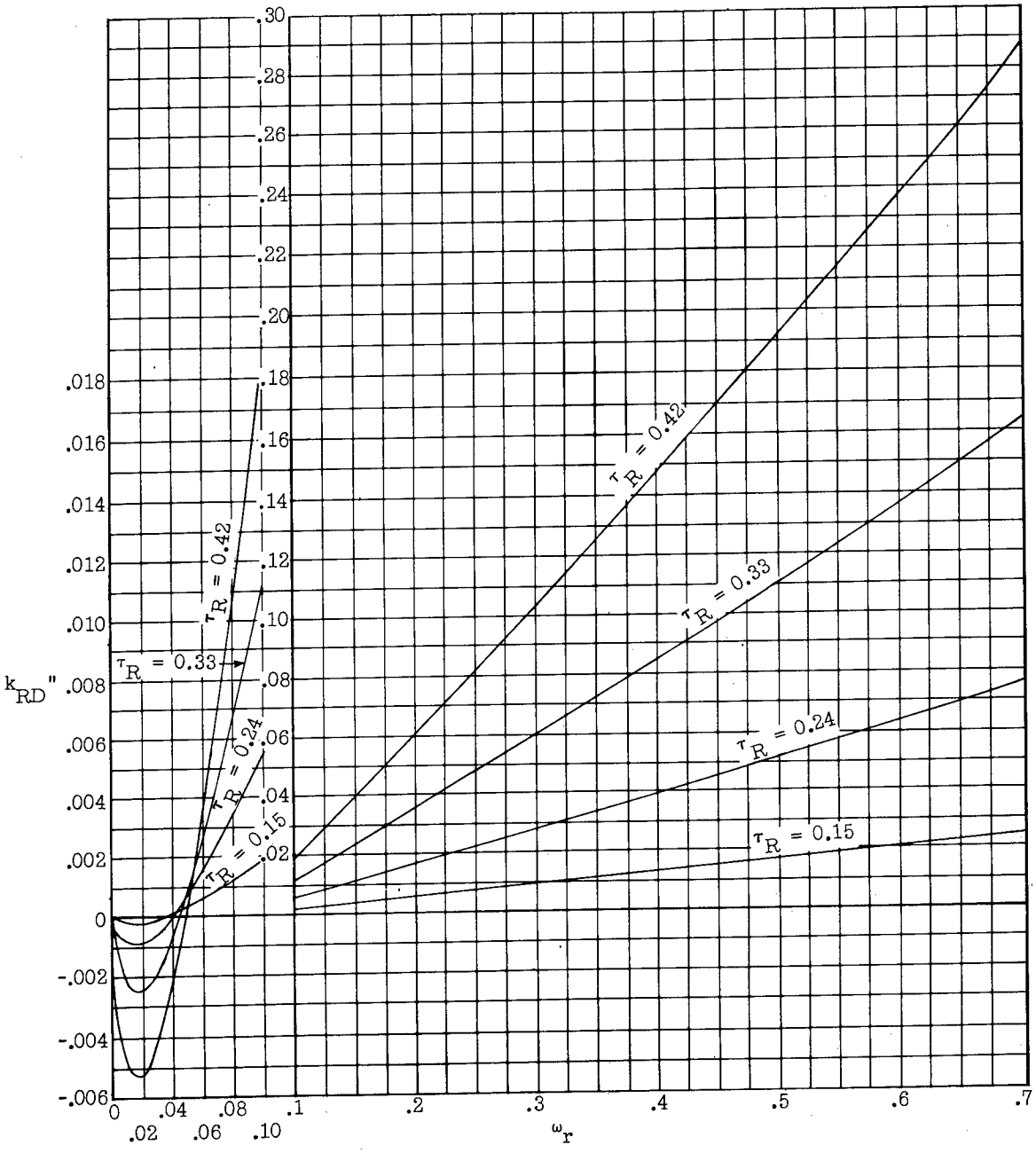

Figure 12.- Imaginary part of k_{RD} for M = 0.7.

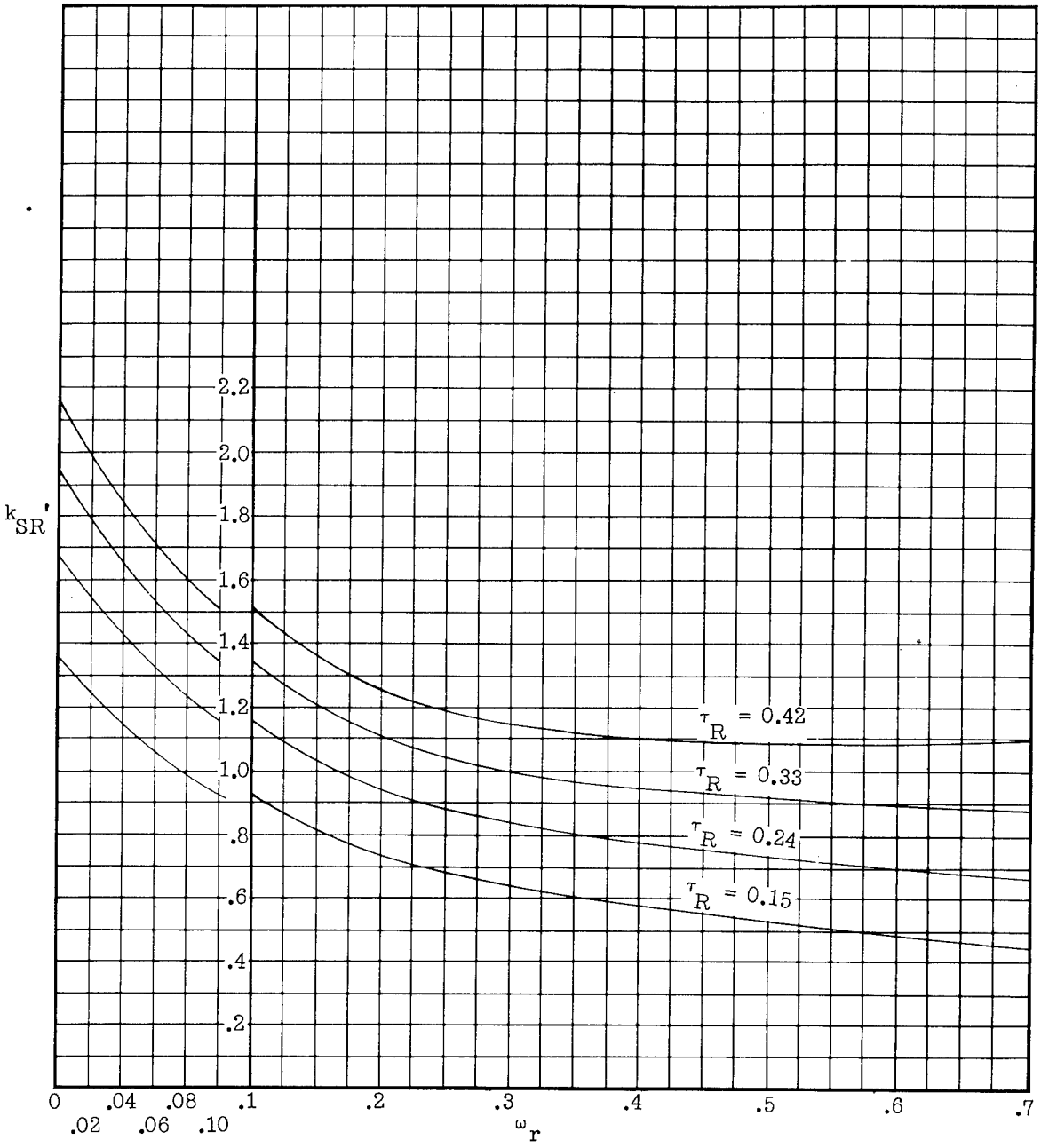

Figure 13.- Real part of k_{SR} for M = 0.7.

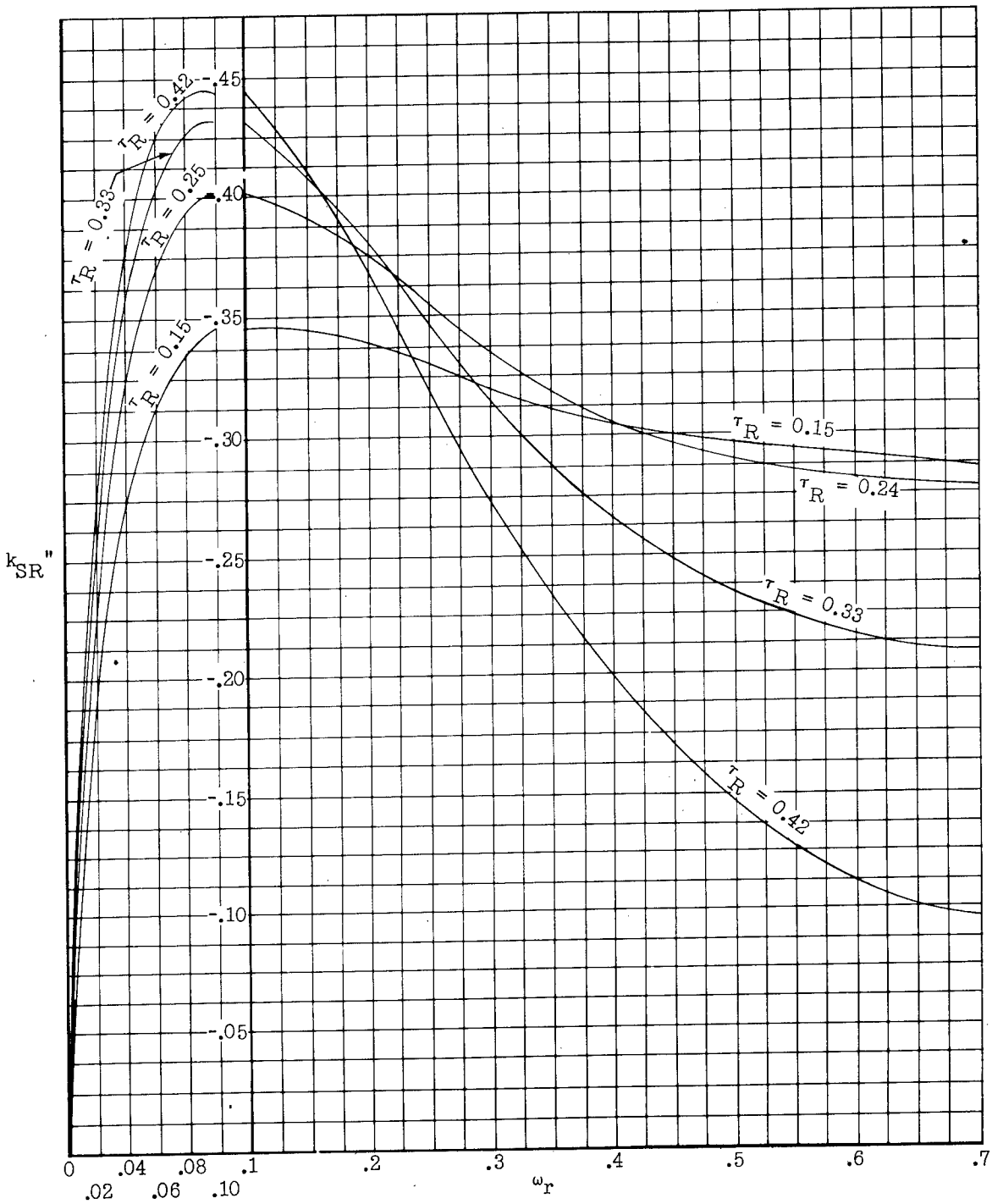

Figure 14.- Imaginary part of k_{SR} for M = 0.7.

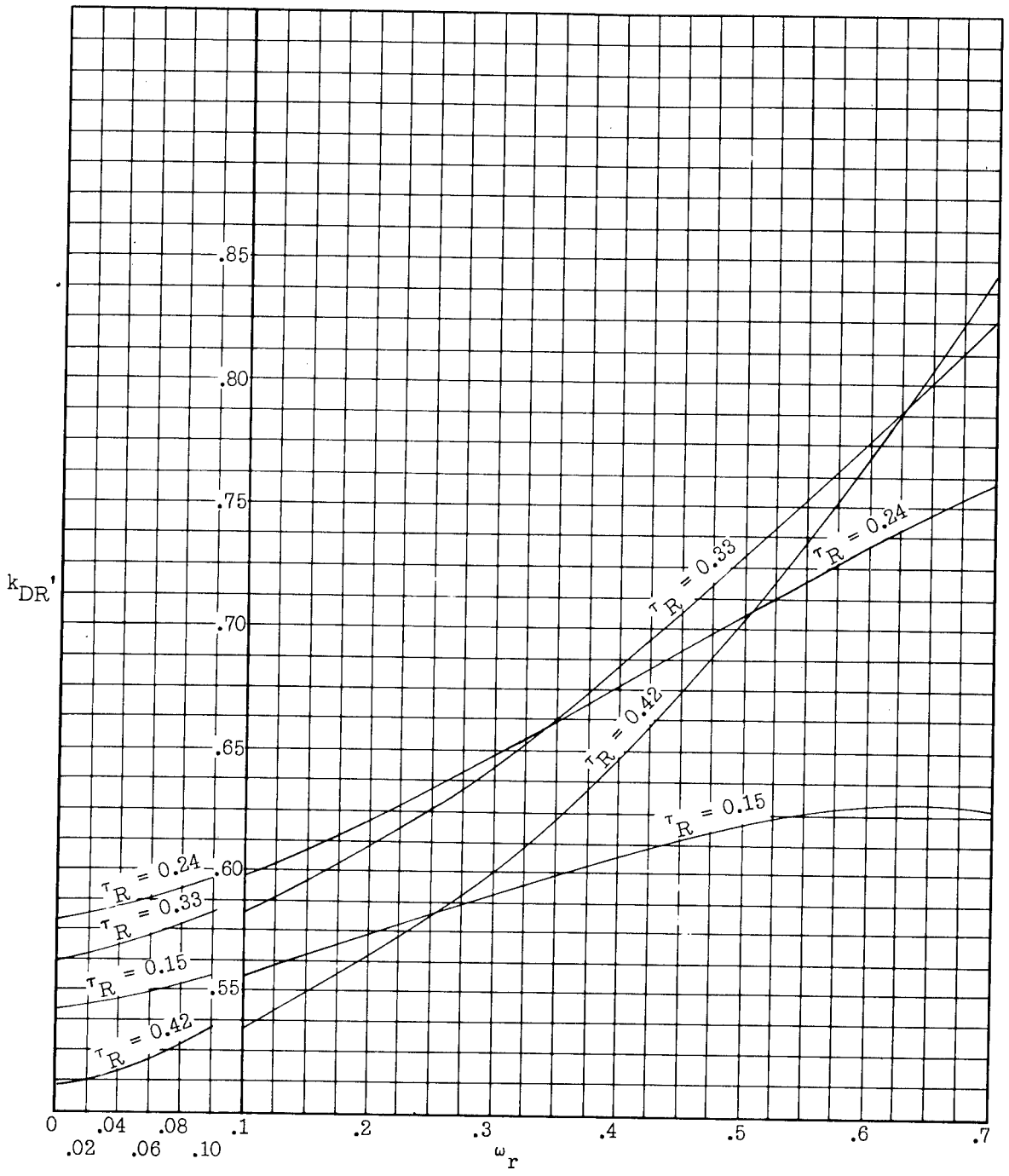

Figure 15.- Real part of k_{DR} for M = 0.7.

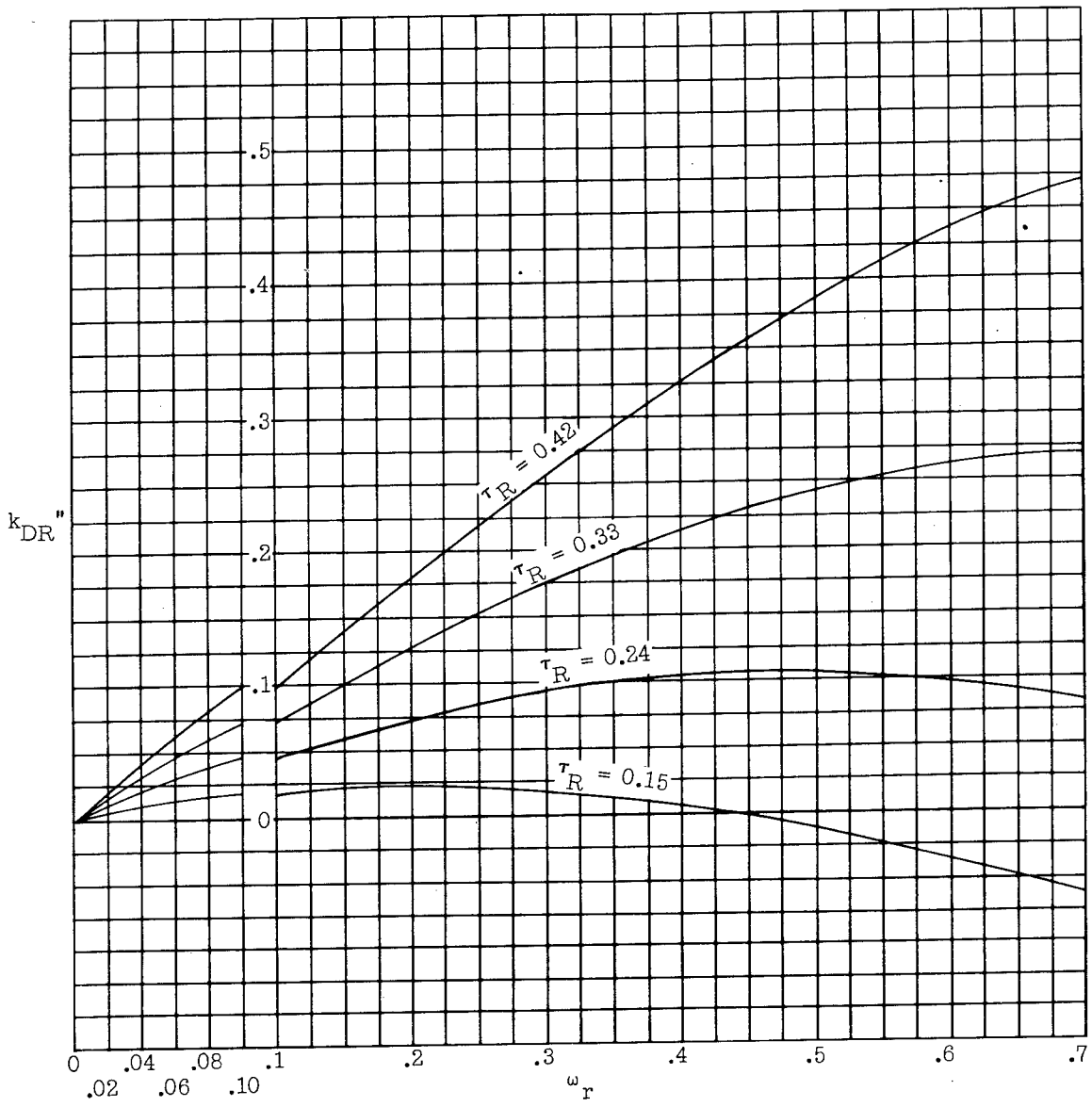

Figure 16.- Imaginary part of k_{DR} for M = 0.7.

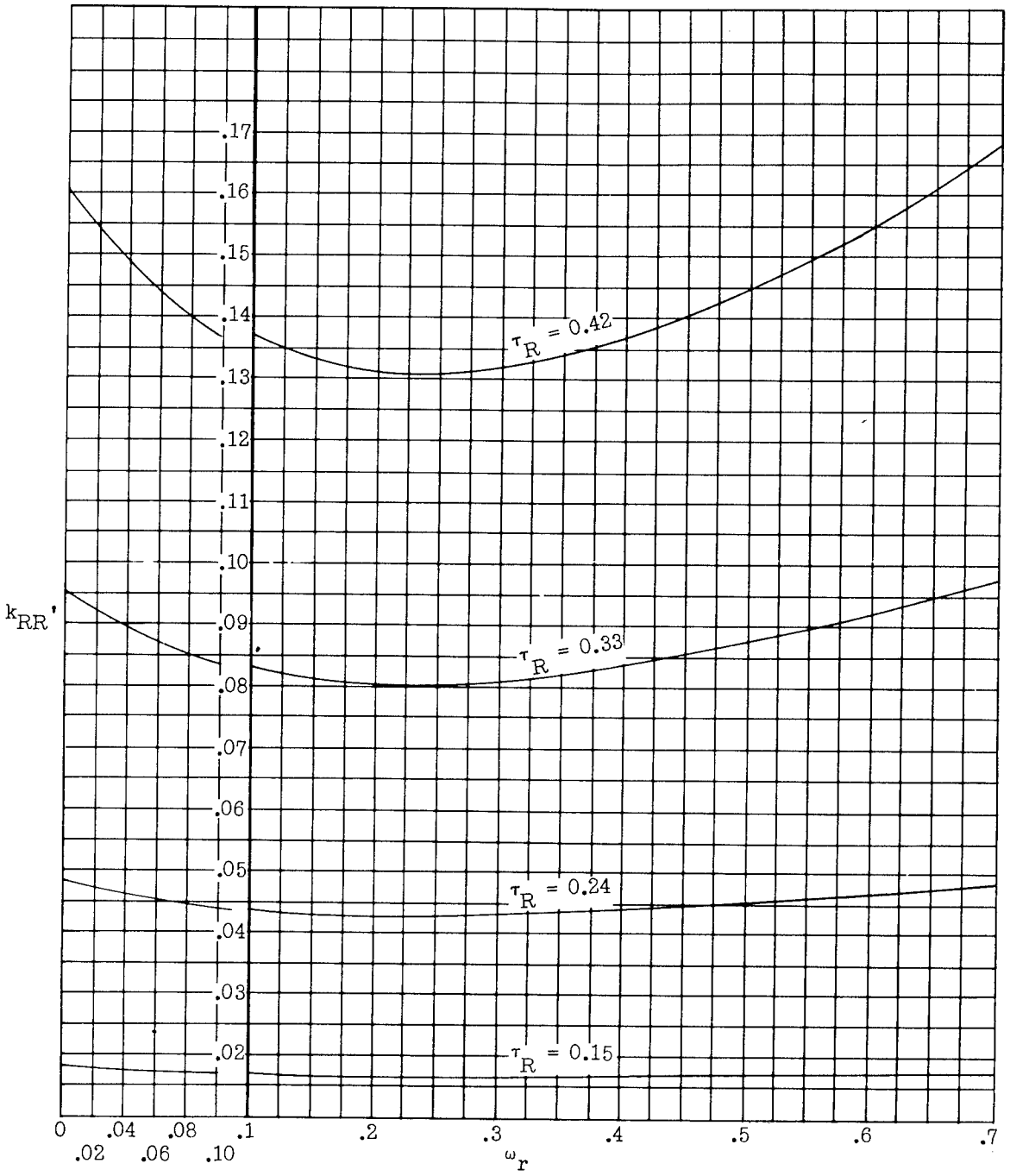

Figure 17.- Real part of k_{RR} for M = 0.7.

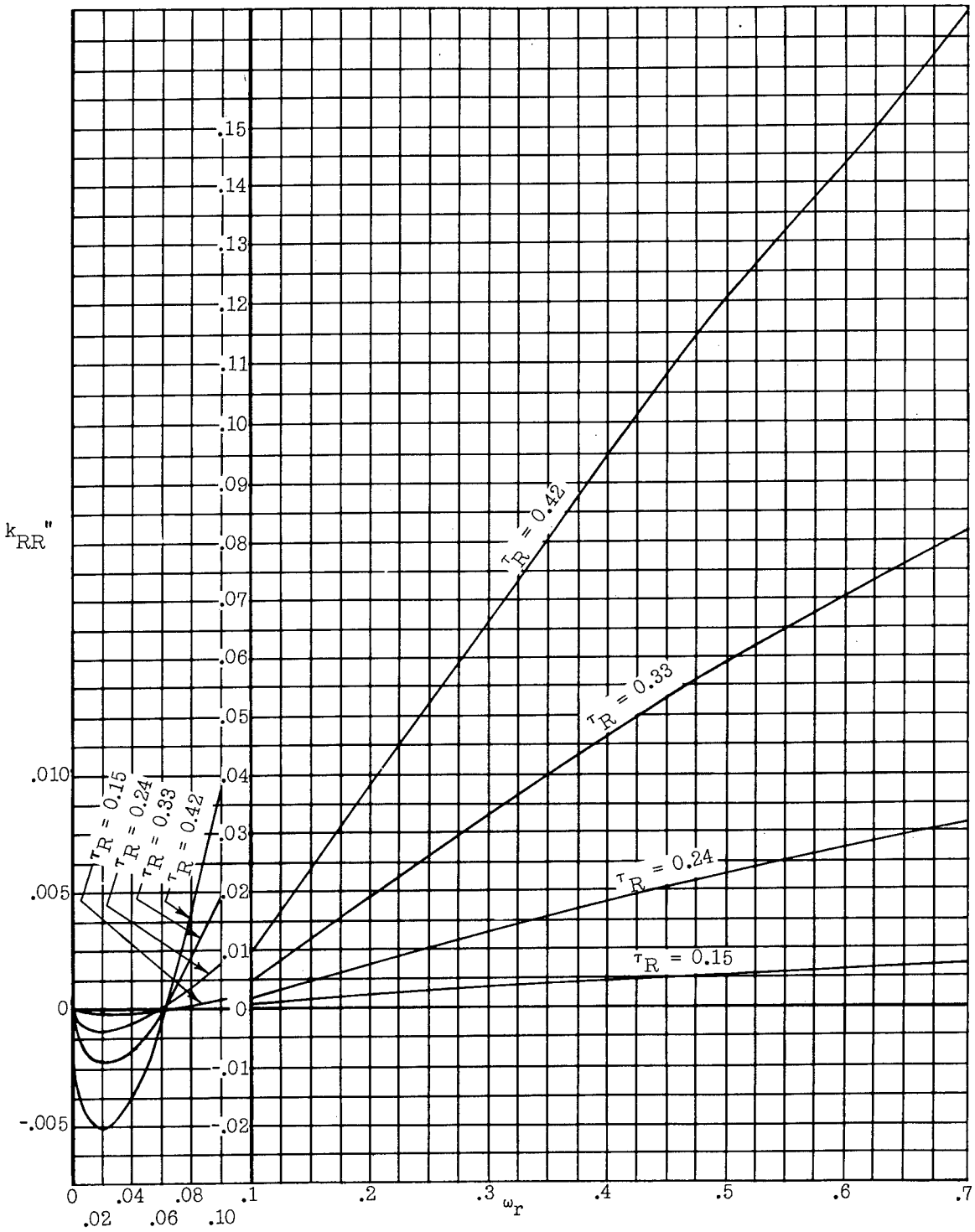

Figure 18.- Imaginary part of k_{RR} for M = 0.7.